Research Article

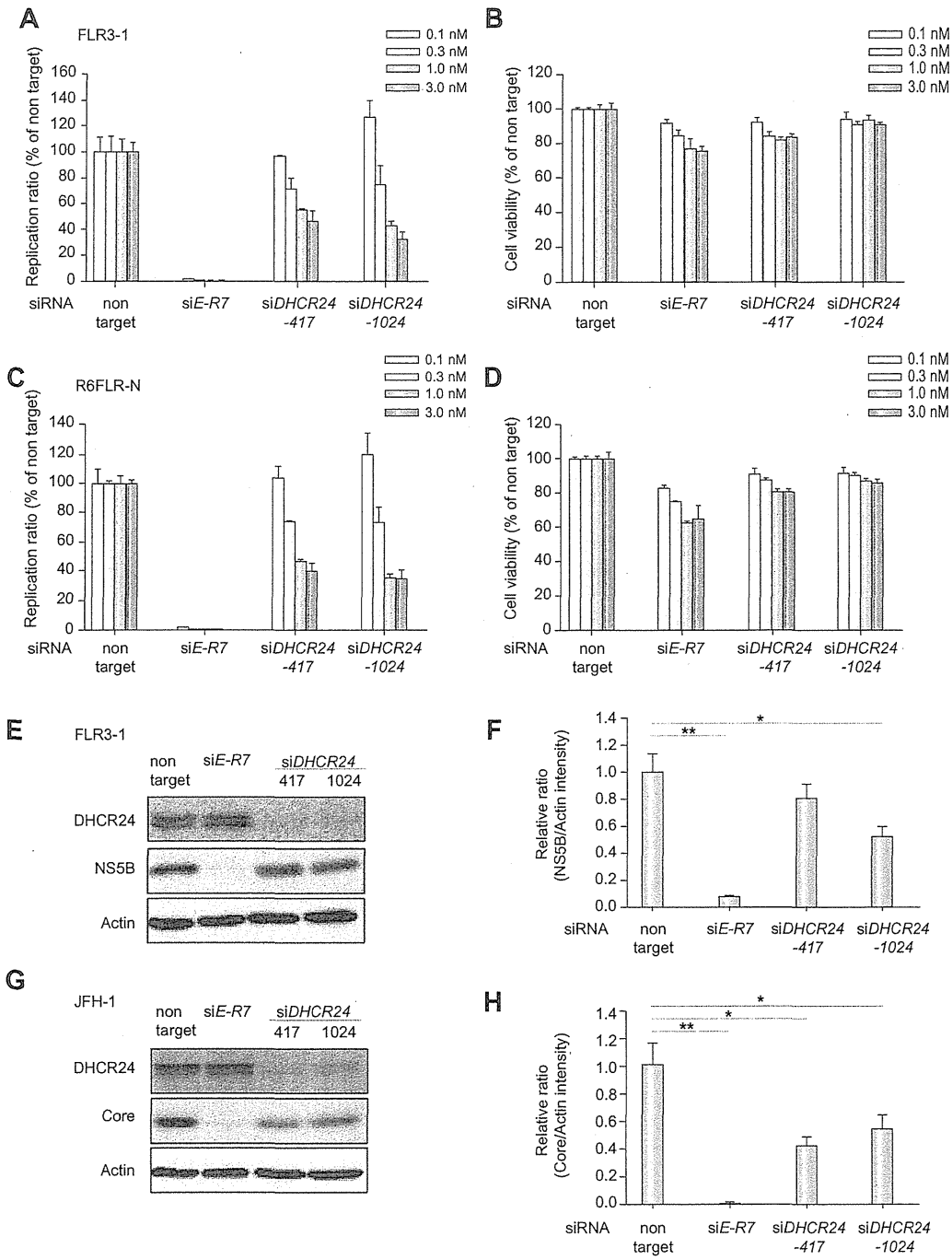

Fig. 2. Effect of DHCR24 knockdown on HCV replication. (A–D) Effect of DHCR24 knockdown on HCV replication in HCV replicon cells (FLR3-1 and R6FLR-N) at 72 h after the anti-*DHCR24* siRNAs (417 and 1024), siRNAs against HCV (siE-R7 for FLR3-1 and JFH-1; siE-R5 for R6-FLR-N), or non-target control siRNAs were transfected into HCV replicon cells. Replication activity was examined by luciferase assay (A and C), and cell viability was measured by the WST-8 assay (B and D). The data represent the mean of three experiments, and the bars indicate SD values. The Western blot analysis (E) and relative intensity of HCV-NS5B protein band was measured by LAS3000 and normalized with that of actin (F) after the treatment with siRNAs targeted against *DHCR24* (siDHCR24-417 and 1024) or HCV (si*E-R7*) in FLR3-1 replicon cells. (G and H) In HCV JFH-1-infected cells, DHCR24 knockdown by si*DHCR*24-417 and 1024 and HCV knockdown by siE-R7 were performed, and DHCR24 and HCV core protein expressions were confirmed by Western blot analysis. The relative intensity ratio of core protein to actin is indicated (H). The data represent the mean of three experiments, and the bars indicate SD values. *p <0.05, **p <0.01 (two-tailed Student's t test).

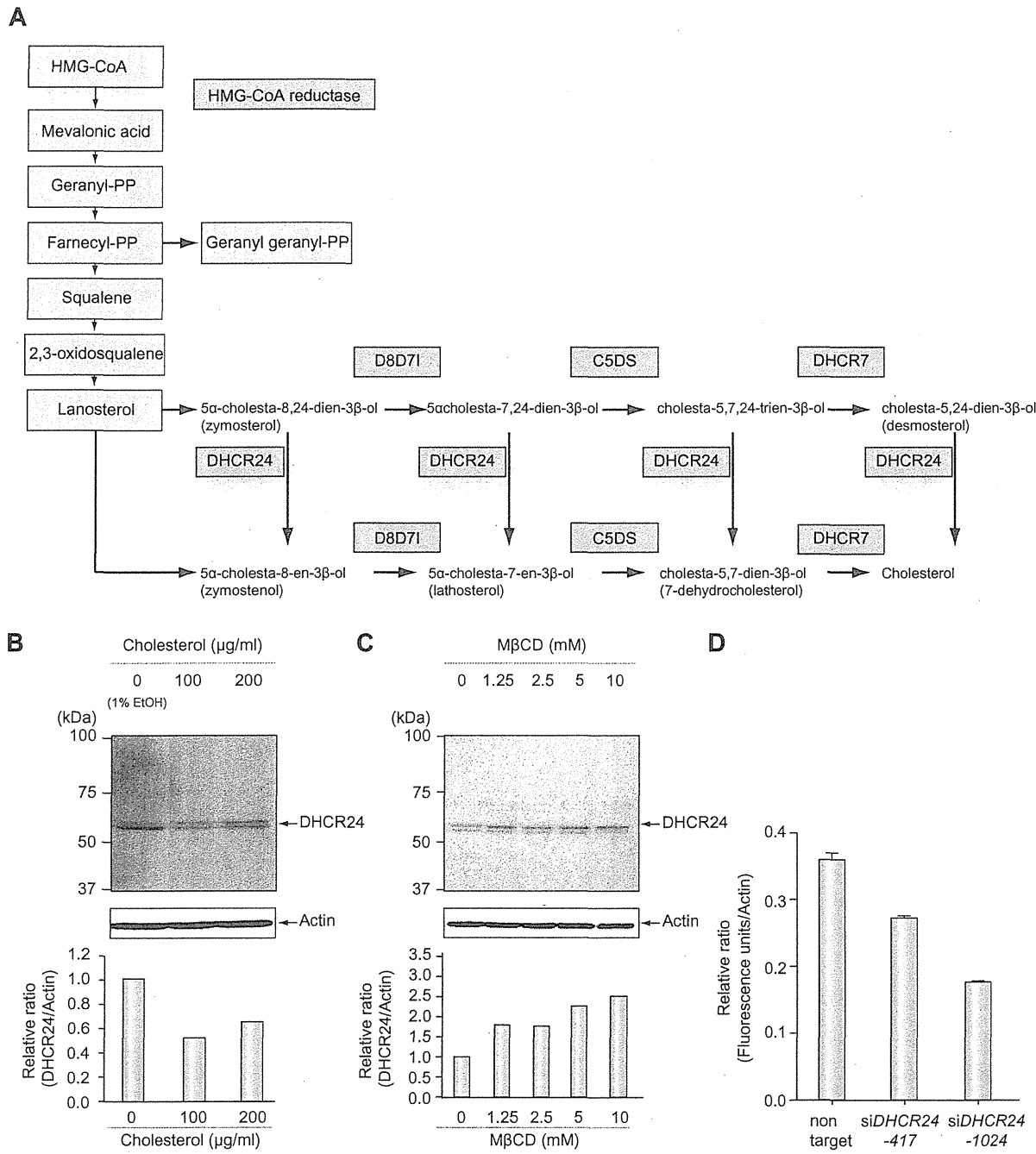

Fig. 3. The level of cholesterol and DHCR24 expression. (A) Cholesterol synthesis pathway, starting from HMG-CoA [26]. The abbreviations used are: D8D7I, 3β-hydroxysterol-delta(8)-delta(7)-isomerase; and C5DS, 3β-hydroxysterol-C^5-desaturase. (B) Cholesterol (0, 100, and 200 μg/ml) was added to HuH-7 cells, and, after 24 h, DHCR24 protein was detected by Western blot analysis using anti-DHCR24 MoAb and protein band intensity was measured and normalized to actin (lower panel). (C) HepG2 cells were treated with MβCD (0, 1.25, 2.5, 5, and 10 mM) for 30 min. After 72 h, these cells were harvested and examined by Western blot analysis with the anti-DHCR24 MoAb and relative intensity was measured as described in (B) (lower panel). (D) Cholesterol concentration in R6FLR-N cells was measured after treatment with non-targeting siRNA and *DHCR24* siRNA (417 and 1024). The cholesterol contents were measured by Amplex Red cholesterol assay, plotted based on fluorescence units and normalized to actin which was measured by Western blot analysis, and the relative ratio was then calculated. The data represent the mean of three experiments, and the bars indicate the SD values.

Research Article

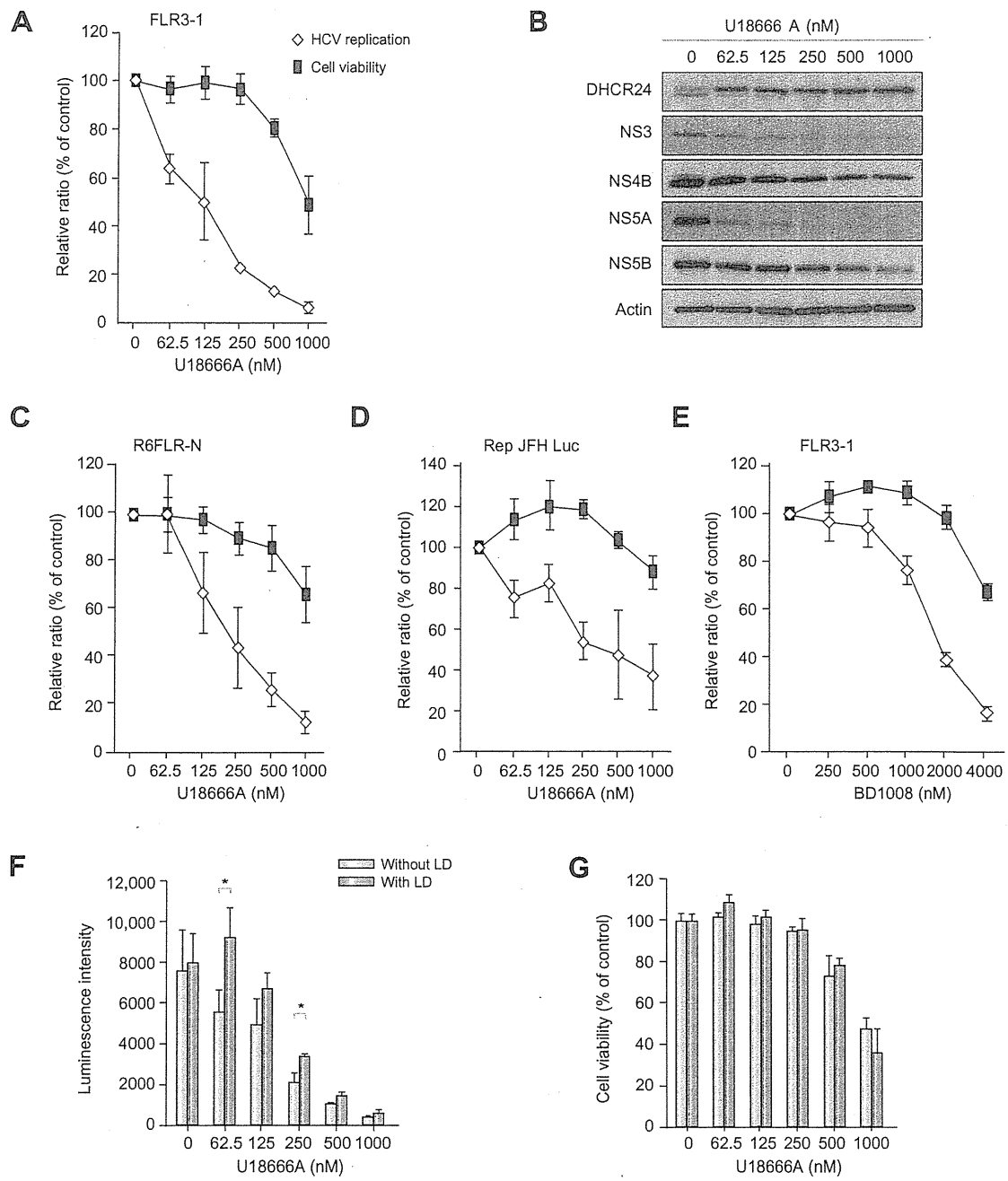

Fig. 4. Effect of U18666A on HCV replication. (A) Addition of U18666A to FLR3-1 cells and subsequent examination of HCV replication by the luciferase assay. Cell viability was measured by WST-8 assay. HCV replication and cell viability were measured 48 h after addition of U18666A. The bars indicate SD values. Open diamonds indicate the relative ratio of viral replication, and black squares indicate the cell viability in relation to untreated controls (A and C–E). (B) Treatment of FLR3-1 cells with U18666A decreased the expression of HCV proteins in a dose-dependent manner, as determined by Western blot analysis. (C and D) Effect of U18666A on HCV replication in other HCV replicon cells (C, R6FLR-N cells; D, Rep JFH Luc 3-13 cells). HCV replication and cell viability analyses were performed as described above. (E) The effect of the DHCR7 inhibitor BD1008 on HCV replicon cells (FLR3-1). Replication activity was examined by the luciferase assay, and cell viability was measured by the WST-8 assay. HCV replication and cell viability analyses were performed 48 h after the addition of U18666A. (F and G) FLR3-1 cells (5×10^3 cells/well) were treated with U18666A alone (light blue, or), low density lipoprotein (LDL) (final cholesterol concentration, 50 μg/ml), and U18666A (dark blue). HCV replication was determined by the luciferase assay 48 h later (F), and cell viability was measured by the WST-8 assay (G). *p <0.05 (two-tailed Student's t-test). The data represent the mean of three experiments, and the bars indicate SD values.

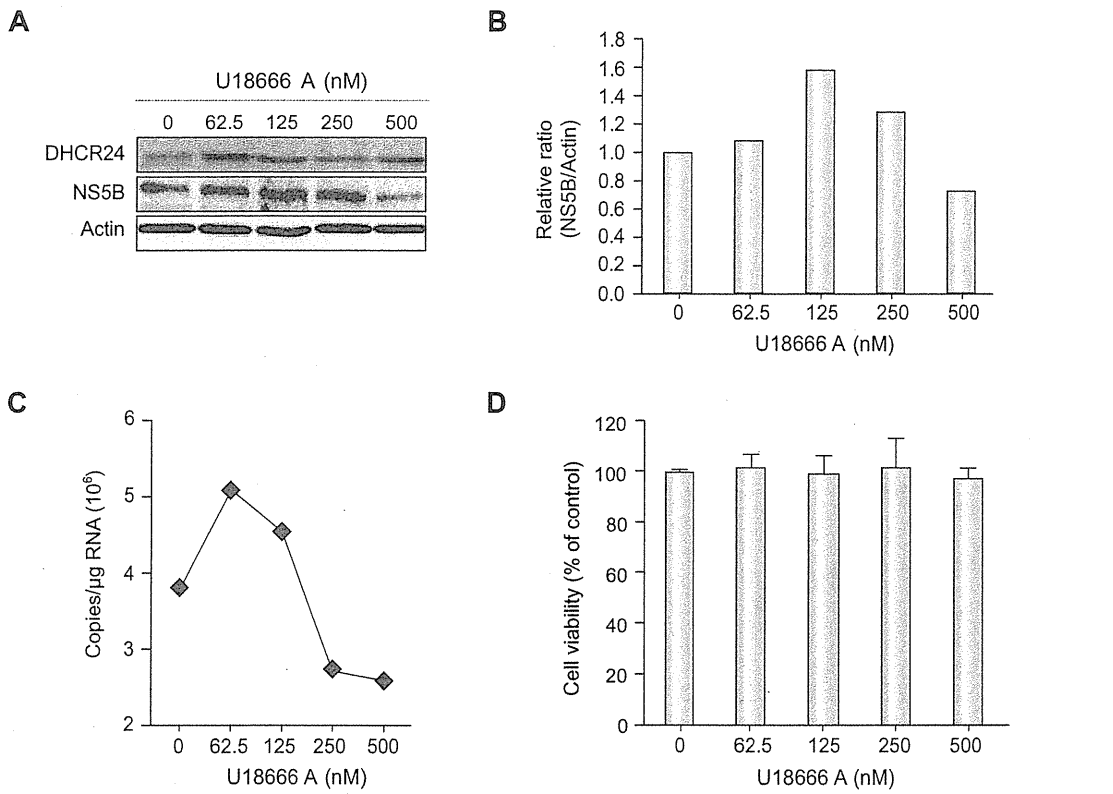

Fig. 5. Effect of U18666A on cells infected with HCV JFH-1. HCV JFH-1-infected cells treated with U18666A were examined 72 h after treatment. (A) Expression of HCV-NS5B protein with or without U18666A treatment, analyzed by Western blot analysis. (B) The intensity of HCV-NS5B protein expression is represented graphically. (C) HCV RNA in HCV JFH-1-infected cells with or without U18666A treatment was measured by RTD-PCR as described in Materials and methods. (D) Cell viability was measured by the WST-8 assay.

HCV replication [28]. The present findings are the first evidence that overexpression of one of the enzymes downstream of the mevalonate pathway, i.e., DHCR24, can be induced by HCV infection. In a previous study, 3-hydroxy 3-methyl-glutaryl Co-A (HMG-CoA) reductase was found to be inhibited by lovastatin, subsequently resulting in suppression of HCV replication [28]. The product of the mevalonate pathway that is required for HCV replication is reported to be a geranyl geranyl lipid [29]. Many lipids are crucial to the viral life cycle, and inhibitors of the cholesterol/fatty acid biosynthetic pathway inhibit viral replication, maturation, and secretion [30,31]. We found that inhibition of DHCR24 down-regulated HCV replication. DHCR24 catalyzes the reduction of the delta-24 bond of the sterol intermediate and works further downstream of farnesyl pyrophosphate (Fig. 3A) and, therefore, does not influence geranyl–geranylation. Thus, our findings indicate the existence of regulatory pathway of HCV replication by cholesterol synthesis and trafficking through DHCR24 rather than by protein geranyl–geranylation. DHCR24 deficiency reduces the cholesterol level and disorganizes cholesterol-rich detergent-resistant membrane domains (DRMs) in mouse brains [32]. Additionally, the HCV replication complex has been detected in the DRM fraction [11]. Therefore, a deficiency in DRM, induced by silencing *DHCR24*, may suppress HCV replication.

We demonstrated that the addition of cholesterol to HCV-infected hepatocytes treated with U18666A led to partial recovery of HCV replication, which suggests that cholesterol may be an important factor in HCV replication. U18666A impairs the intracellular biosynthesis and transport of cholesterol and inhibits the action of membrane-bound enzymes, including DHCR24, during sterol synthesis [33]. Moreover, the DHCR7 inhibitor BD1008 also suppresses HCV replication. Thus, the findings in this study further substantiate the fact that cholesterol plays an important role in HCV replication and infection.

Although monotherapy with statins is reportedly insufficient to induce anti-viral activity in HCV-infected patients [34], a synergistic action between statins and IFN has been observed [35]. The effect of the statin is thought to be mainly mediated by the depletion of geranyl geranyl lipids. It is important to note that higher doses of statins may increase the risk of myopathy, liver dysfunction, and cardiovascular events [36]. Moreover, the EC_{50} values of the statins that are associated with a reduction in HCV replication are reported to be 0.45–2.16 μM, while the IC_{50} of U18666A was estimated to be 125 nM in the present study. Therefore, U18666A may serve as a novel anti-HCV drug that could be utilized with IFN as a combined therapeutic regimen.

In summary, we demonstrated that the expression of DHCR24 is induced by infection with HCV and that DHCR24 is an essential host factor that is required for HCV replication. HCV may increase cholesterol synthesis in cells via the action of a host regulatory factor, such as DHCR24, that is correlated with cholesterol

Research Article

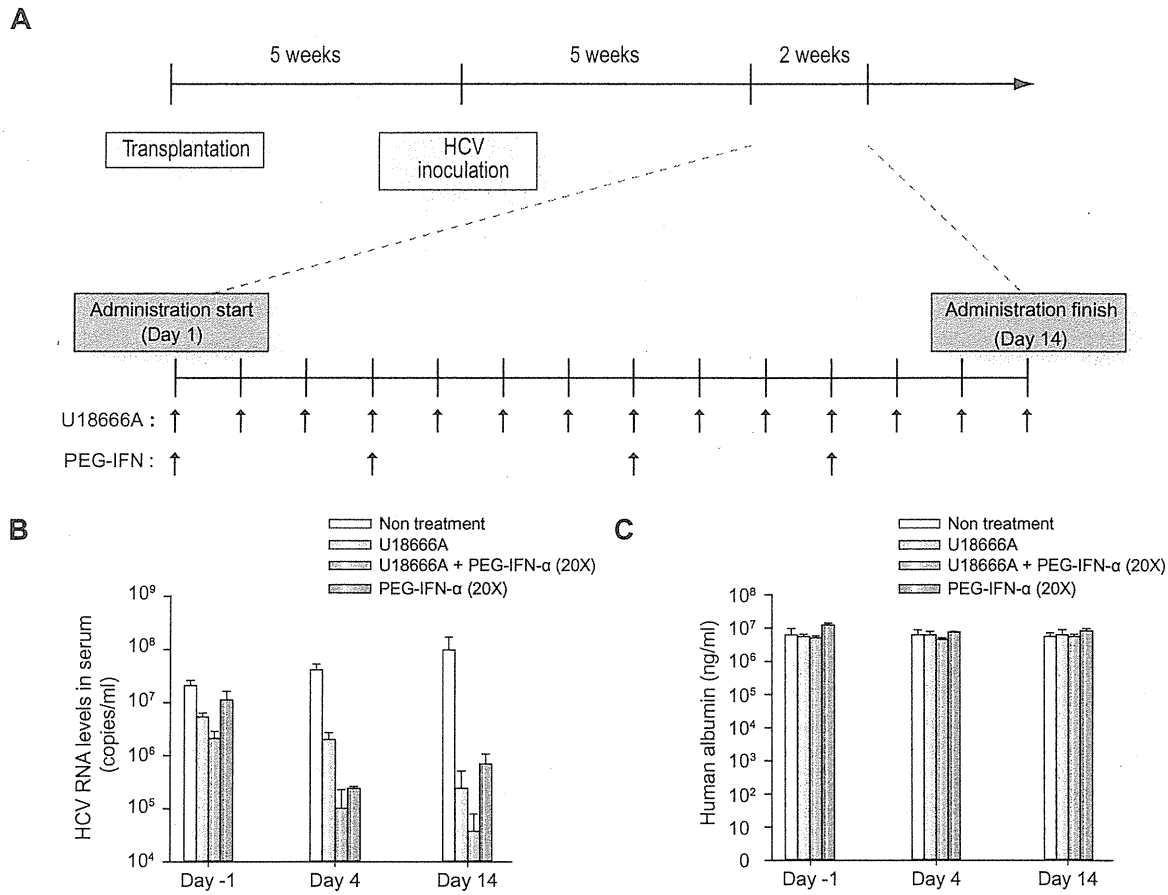

Fig. 6. Evaluation of the anti-HCV effect of U18666A in chimeric mice. (A) Diagram of the schedule that was followed to produce chimeric mice with the humanized liver, perform blood sampling, and administer drugs to chimeric mice infected with HCV. Four groups of three chimeric mice with the humanized liver were treated intraperitoneally with U18666A (10 mg/kg) and/or subcutaneously with PEG-IFN-α (30 μg/kg) at 2-day intervals for 2 weeks. (B) The effect of U18666A and/or PEG-IFN-α on HCV replication in chimeric mice with the humanized liver was determined by quantification of HCV-RNA using RTD-PCR. The bars indicate SD values ($n = 12$). (C) Human albumin concentrations in the sera of chimeric mice with the humanized liver. The bars indicate SD values ($n = 12$).

synthesis and is also directly involved in replication. Genome-wide analysis of the host response to HCV infection revealed the upregulation of genes related to lipid metabolism [37]. DHCR24 expression was found to be upregulated in the cDNA microarray analysis of chronic hepatitis C cases [38]. Future studies are needed to examine the detailed mechanism by which HCV infection augments DHCR24 expression in hepatocytes.

Conflict of interest

The authors who have taken part in this study declared that they do not have anything to disclose regarding funding or conflict of interest with respect to this manuscript.

Financial support

This study was supported in part by a grant from the Ministry of Education, Culture, Sports, Science and Technology of Japan, a grant from the Ministry of Health, Labor and Welfare of Japan, and the Program for Promotion of Fundamental Studies in Health Sciences of the National Institute of Biomedical Innovation of Japan and the Cooperative Research Project on Clinical and Epidemiological Studies of Emerging and Re-emerging Infectious Diseases.

Acknowledgments

We are very grateful to Dr. T. Watanabe, Dr. S. Nakagawa, Mr. T. Nishimura and Dr. K. Tanaka for technical support, and Dr. S. To'ne, Dr. T. Wakita, Dr. S. Sekiguchi, and Dr. F. Yasui for helpful discussions.

Supplementary data

Supplementary data associated with this article can be found, in the online version, at doi:10.1016/j.jhep.2010.12.011.

References

[1] Llovet JM, Burroughs A, Bruix J. Hepatocellular carcinoma. Lancet 2003;362:1907–1917.

[2] Tsukuma H, Hiyama T, Tanaka S, et al. Risk factors for hepatocellular carcinoma among patients with chronic liver disease. N Engl J Med 1993;328:1797–1801.

[3] Wasley A, Alter MJ. Epidemiology of hepatitis C: geographic differences and temporal trends. Semin Liver Dis 2000;20:1–16.

[4] Kohara M, Tanaka T, Tsukiyama-Kohara K, et al. Hepatitis C virus genotypes 1 and 2 respond to interferon-alpha with different virologic kinetics. J Infect Dis 1995;172:934–938.

[5] Tsukiyama-Kohara K, Tone S, Maruyama I, et al. Activation of the CKI-CDK-Rb-E2F pathway in full genome hepatitis C virus-expressing cells. J Biol Chem 2004;279:14531–14541.

[6] Nishimura T, Kohara M, Izumi K, et al. Hepatitis C virus impairs p53 via persistent overexpression of 3beta-hydroxysterol Delta24-reductase. J Biol Chem 2009;284:36442–36452.

[7] Greeve I, Hermans-Borgmeyer I, Brellinger C, et al. The human DIMINUTO/DWARF1 homolog seladin-1 confers resistance to Alzheimer's disease-associated neurodegeneration and oxidative stress. J Neurosci 2000;20:7345–7352.

[8] Wu C, Miloslavskaya I, Demontis S, Maestro R, Galaktionov K. Regulation of cellular response to oncogenic and oxidative stress by Seladin-1. Nature 2004;432:640–645.

[9] Waterham HR, Koster J, Romeijn GJ, et al. Mutations in the 3beta-hydroxysterol Delta24-reductase gene cause desmosterolosis, an autosomal recessive disorder of cholesterol biosynthesis. Am J Hum Genet 2001;69:685–694.

[10] Wechsler A, Brafman A, Shafir M, et al. Generation of viable cholesterol-free mice. Science 2003;302:2087.

[11] Aizaki H, Lee KJ, Sung VM, Ishiko H, Lai MM. Characterization of the hepatitis C virus RNA replication complex associated with lipid rafts. Virology 2004;324:450–461.

[12] Di Stasi D, Vallacchi V, Campi V, et al. DHCR24 gene expression is upregulated in melanoma metastases and associated to resistance to oxidative stress-induced apoptosis. Int J Cancer 2005;115:224–230.

[13] Bierkamper GG, Cenedella RJ. Induction of chronic epileptiform activity in the rat by an inhibitor of cholesterol synthesis, U18666A. Brain Res 1978;150:343–351.

[14] Nakabayashi H, Taketa K, Miyano K, Yamane T, Sato J. Growth of human hepatoma cells lines with differentiated functions in chemically defined medium. Cancer Res 1982;42:3858–3863.

[15] Knowles BB, Howe CC, Aden DP. Human hepatocellular carcinoma cell lines secrete the major plasma proteins and hepatitis B surface antigen. Science (New York, NY) 1980;209:497–499.

[16] Sakamoto H, Okamoto K, Aoki M, et al. Host sphingolipid biosynthesis as a target for hepatitis C virus therapy. Nat Chem Biol 2005;1:333–337.

[17] Watanabe T, Sudoh M, Miyagishi M, et al. Intracellular-diced dsRNA has enhanced efficacy for silencing HCV RNA and overcomes variation in the viral genotype. Gene Ther 2006;13:883–892.

[18] Wakita T, Pietschmann T, Kato T, et al. Production of infectious hepatitis C virus in tissue culture from a cloned viral genome. Nat Med 2005;11:791–796.

[19] Inoue K, Umehara T, Ruegg UT, et al. Evaluation of a cyclophilin inhibitor in hepatitis C virus-infected chimeric mice in vivo. Hepatology 2007;45:921–928.

[20] Jensen ON, Wilm M, Shevchenko A, Mann M. Sample preparation methods for mass spectrometric peptide mapping directly from 2-DE gels. Methods Mol Biol (Clifton, NJ) 1999;112:513–530.

[21] Nakagawa S, Umehara T, Matsuda C, et al. Hsp90 inhibitors suppress HCV replication in replicon cells and humanized liver mice. Biochem Biophys Res Commun 2007;353:882–888.

[22] Takeuchi T, Katsume A, Tanaka T, et al. Real-time detection system for quantification of hepatitis C virus genome. Gastroenterology 1999;116:636–642.

[23] Mercer DF, Schiller DE, Elliott JF, et al. Hepatitis C virus replication in mice with chimeric human livers. Nat Med 2001;7:927–933.

[24] Tateno C, Yoshizane Y, Saito N, et al. Near completely humanized liver in mice shows human-type metabolic responses to drugs. Am J Pathol 2004;165:901–912.

[25] Umehara T, Sudoh M, Yasui F, et al. Serine palmitoyltransferase inhibitor suppresses HCV replication in a mouse model. Biochem Biophys Res Commun 2006;346:67–73.

[26] Kedjouar B, de Medina P, Oulad-Abdelghani M, et al. Molecular characterization of the microsomal tamoxifen binding site. J Biol Chem 2004;279:34048–34061.

[27] John CS, Lim BB, Geyer BC, Vilner BJ, Bowen WD. 99mTc-labeled sigma-receptor-binding complex: synthesis, characterization, and specific binding to human ductal breast carcinoma (T47D) cells. Bioconjug Chem 1997;8:304–309.

[28] Ye J, Wang C, Sumpter Jr R, et al. Disruption of hepatitis C virus RNA replication through inhibition of host protein geranyl-geranylation. Proc Natl Acad Sci USA 2003;100:15865–15870.

[29] Kapadia SB, Chisari FV. Hepatitis C virus RNA replication is regulated by host geranyl-geranylation and fatty acids. Proc Natl Acad Sci USA 2005;102:2561–2566.

[30] Aizaki H, Morikawa K, Fukasawa M, et al. Critical role of virion-associated cholesterol and sphingolipid in hepatitis C virus infection. J Virol 2008;82:5715–5724.

[31] Syed GH, Amako Y, Siddiqui A. Hepatitis C virus hijacks host lipid metabolism. Trends Endocrinol Metab 2010;21:33–40.

[32] Crameri A, Biondi E, Kuehnle K, et al. The role of seladin-1/DHCR24 in cholesterol biosynthesis, APP processing and Abeta generation in vivo. EMBO J 2006;25:432–443.

[33] Cenedella RJ. Cholesterol synthesis inhibitor U18666A and the role of sterol metabolism and trafficking in numerous pathophysiological processes. Lipids 2009;44:477–487.

[34] Bader T, Fazili J, Madhoun M, et al. Fluvastatin inhibits hepatitis C replication in humans. Am J Gastroenterol 2008;103:1383–1389.

[35] Ikeda M, Abe K, Yamada M, et al. Different anti-HCV profiles of statins and their potential for combination therapy with interferon. Hepatology (Baltimore, MD) 2006;44:117–125.

[36] Argo CK, Loria P, Caldwell SH, Lonardo A. Statins in liver disease: a molehill, an iceberg, or neither? Hepatology (Baltimore, MD) 2008;48:662–669.

[37] Su AI, Pezacki JP, Wodicka L, et al. Genomic analysis of the host response to hepatitis C virus infection. Proc Natl Acad Sci USA 2002;99:15669–15674.

[38] Honda M, Yamashita T, Ueda T, et al. Different signaling pathways in the livers of patients with chronic hepatitis B or chronic hepatitis C. Hepatology 2006;44:1122–1138.

Virus Research 160 (2011) 89–97

Contents lists available at ScienceDirect

Virus Research

journal homepage: www.elsevier.com/locate/virusres

Conditional gene expression in hepatitis C virus transgenic mice without induction of severe liver injury using a non-inflammatory Cre-expressing adenovirus

Tomoko Chiyo[a], Satoshi Sekiguchi[a], Masahiro Hayashi[a], Yoshimi Tobita[a], Yumi Kanegae[b], Izumu Saito[b], Michinori Kohara[a,*]

[a] Department of Microbiology and Cell Biology, The Tokyo Metropolitan Institute of Medical Science, 1-6, Kamikitazawa 2-chome, Setagaya-ku, Tokyo 156-8505, Japan
[b] Laboratory of Molecular Genetics, Institute of Medical Science, The University of Tokyo, Tokyo 108-8639, Japan

ARTICLE INFO

Article history:
Received 29 December 2010
Received in revised form 19 May 2011
Accepted 20 May 2011
Available online 30 May 2011

Keywords:
HCV transgenic mouse
Cre/loxP system
Recombinant adenovirus vector
EF1α promoter
Hepatitis

ABSTRACT

We previously established inducible-hepatitis C virus (HCV) transgenic mice, which expressed the HCV gene (nucleotides 294–3435) encoding the core, E1, E2, and NS2 proteins. The expression of these proteins is regulated by the Cre/loxP system and an adenovirus vector (AdV) that expresses Cre DNA recombinase (Cre) controlled by the CAG promoter (AxCANCre). Recent studies have demonstrated that AxCANCre injection alone results in severe liver injury by induction of the adenovirus protein IX (Ad-pIX) gene. As a result, HCV protein expression in transgenic mice livers was only short-term. In contrast, the EF1α promoter-bearing AdV induces slight Ad-pIX gene expression without inducing severe liver injury. Therefore, in the present study, we developed a Cre-expressing AdV that bears the EF1α promoter (AxEFCre) to express HCV protein in the transgenic mouse livers. In the non-transgenic mice injected with AxCANCre, alanine aminotransferase (ALT) levels were elevated and severe liver inflammation occurred; this was not observed in AxEFCre-injected mice. In contrast, AxEFCre-injected HCV transgenic mice showed milder liver inflammatory responses that were clearly due to HCV protein expression. Moreover, the AxEFCre injection enabled the transgenic mice to persistently express HCV protein. These results indicate that use of AxEFCre efficiently promotes Cre-mediated DNA recombination *in vivo* without a severe hepatitis response to AdV. This inducible-HCV transgenic mouse model using AxEFCre should be useful for research on HCV pathogenesis.

1. Introduction

Infection with the hepatitis C virus (HCV) is a major global health problem, as persistent viral infection leads to liver cirrhosis and hepatocellular carcinoma (Goodman and Ishak, 1995; Shepard et al., 2005). The chimpanzee is the only validated animal model for *in vivo* studies of HCV infection, while *in vivo* studies on the pathogenesis of HCV have been conducted using new animal models (Kremsdorf and Brezillon, 2007). Several groups have established transgenic mice that constitutively express single or multiple HCV protein(s) in the liver (Lerat et al., 2002; Moriya et al., 1997). However, in these mice, HCV protein expression begins *in utero*; as a result, they develop immune tolerance to the HCV antigens, and HCV-specific cellular responses or liver inflammation cannot be induced. To overcome these obstacles, we previously developed immunocompetent HCV transgenic mice in which HCV protein expression was tightly regulated by the Cre/*lox*P system (Wakita et al., 1998).

The E1- and E3-deleted adenovirus vector (AdV) has been widely used for both basic studies of gene function and for gene therapy *in vivo*. To deliver the *Cre* gene into the livers of HCV transgenic mice, we used an AdV that carries the CAG promoter linked to a nuclear localization signal-tagged Cre (AxCANCre), which has been used for Cre-mediated DNA recombination (Baba et al., 2005; Kobayashi et al., 2000; Shintani et al., 1999; Wakita et al., 1998). While AdV is relatively efficient in inducing transgene expression, several studies have shown that the viral vector itself can induce strong inflammatory responses in murine livers (Kafri et al., 1998; Wakita et al., 2000). Moreover, expression of transgenes via AdVs persists for only 2–4 weeks due to elimination of infected cells through immune responses directed against the AdVs (Akagi et al., 1997; Bangari and Mittal, 2006; Kafri et al., 1998; Sun et al., 2005; Wakita et al., 2000). To address these problems, the viral

* Corresponding author. Tel.: +81 3 5316 3232; fax: +81 3 5316 3137.
E-mail addresses: chiyo-tm@ncnp.go.jp (T. Chiyo), sekiguchi-st@igakuken.or.jp (S. Sekiguchi), mahayashi-kyt@umin.ac.jp (M. Hayashi), tobita-ys@igakuken.or.jp (Y. Tobita), kanegae@ims.u-tokyo.ac.jp (Y. Kanegae), isaito@ims.u-tokyo.ac.jp (I. Saito), kohara-mc@igakuken.or.jp (M. Kohara).

0168-1702/$ – see front matter © 2011 Elsevier B.V. All rights reserved.
doi:10.1016/j.virusres.2011.05.019

genes that cause cellular immune responses have been investigated. Recently, Nakai et al. (2007) reported that co-expression of adenovirus protein IX (Ad-pIX) resulted in AdV-induced immune responses. However, AdVs that carried the EF1α promoter did not induce Ad-pIX or increase the alanine aminotransferase (ALT) level, facilitating long-term transgene expression in mice.

In the present study, we generated a Cre-expressing AdV bearing the EF1α promoter (AxEFCre) to enable the persistent expression of HCV protein in the livers of inducible-HCV transgenic mice regulated by the Cre/*lox*P recombination system. When this AdV was used to express Cre in the HCV transgenic mouse livers, it induced less severe inflammatory responses and improved the long-term expression of HCV proteins compared to CAG promoter-bearing AdVs. Thus, AxEFCre efficiently promotes Cre-mediated DNA recombination *in vivo* without a severe hepatitis response to AdV and should be useful for HCV gene expression in the HCV transgenic mice.

2. Materials and methods

2.1. Cells

The 293 cells [CRL-1573, a human embryonic kidney cell line that contains the Ad5 E1 region; American Type Culture Collection (ATCC)] and HepG2 cells (HB-8065, a human hepatocellular carcinoma cell line; ATCC) were maintained in Dulbecco's modified Eagle's medium (DMEM; Nissui Pharmaceutical) supplemented with 10% fetal bovine serum (FBS; JRH Biosciences), 100 U/mL penicillin, and 100 μg/mL streptomycin (GIBCO) (10% FBS-DMEM). In addition, HepG2 cells containing the Cre reporter unit CALNLZ (Baba et al., 2005), termed Hep-CALNLZ cells, were selected for resistance to G418 (300 μg/mL; Sigma) and cultured in 10% FBS-DMEM.

2.2. Adenovirus vectors

E1- and E3-deleted AdVs derived from human adenovirus type 5 encoding expression units with a leftward orientation were used in this study. As expression units, untagged Cre or NLS-tagged Cre under the control of the CAG promoter (AxCANCre or AxCACre), untagged Cre or NLS-tagged Cre under the control of the EF1α promoter (AxEFNCre or AxEFCre), and untagged β-galactosidase (LacZ) under the control of the EF1α promoter (AxEFLacZ) were constructed (Fig. 1A). AxCANCre and AxCACre were generated as described previously (Kanegae et al., 1995). AxEFNCre, AxEFCre, and AxEFLacZ were constructed using pAxEFwtit2 DNA/RE Treatment (Nippon Gene). All of the AdVs were purified using two rounds of CsCl gradient centrifugation, and the titers of the concentrated and purified virus stocks were determined as described previously (Kanegae et al., 1994).

2.3. Animal procedures

HCV transgenic mice CN2-29 (C57BL/6 background) and normal C57BL/6 mice were used in the experiments. The CN2-29 transgenic mice express HCV genotype 1b proteins (core, E1, E2, and NS2 proteins) under the regulation of the Cre/*lox*P conditional switching system (Wakita et al., 1998). The transgenic mice were intravenously injected with each AdV at a dose of 1.0×10^9 plaque-forming units (PFU), and sacrificed 0.5, 7, or 21 days after injection for liver histology and biochemical analysis. All mice were bred in a pathogen-free facility and tested routinely for mouse hepatitis virus and other pathogens. All experiments using mice were approved by The Tokyo Metropolitan Institute of Medical Science Animal Experiment Committee and were performed in accordance with the animal experimentation guidelines of The Tokyo Metropolitan Institute of Medical Science.

2.4. Western blot detection of Cre and Ad-pIX

The HepG2 cells were placed in collagen-coated, 12-well plates and infected with the AdVs at a multiplicity of infection (MOI) of 20 or 100 for Western blot detection of Cre or Ad-pIX, respectively. After 24 h, the cells were washed with phosphate-buffered saline (PBS) and resolved in radioimmunoprecipitation assay (RIPA) buffer [10 mM Tris–HCl (pH 7.5), 0.15 M NaCl, 1% sodium dodecyl sulfate (SDS), 0.5% Nonidet P-40, protease inhibitor cocktail (Complete; Roche Molecular Biochemicals)]. The protein concentrations of the cell lysates were measured using the DC protein assay (Bio-Rad Laboratories). The cell lysates were electrophoresed on SDS–polyacrylamide gel, transferred to polyvinylidene difluoride membrane (GE Healthcare) activated with methanol, and blocked with 5% skim milk in PBS containing 0.1% Tween-20 (PBST). After washing with PBST, the membrane was incubated overnight at 4 °C in the presence of anti-Cre rabbit polyclonal antibody or anti-Ad-pIX rabbit polyclonal antibody (Nakai et al., 2007) prepared from hyper-immune rabbit sera, or anti-β-actin mouse monoclonal antibody (Sigma), followed by incubation with horseradish peroxidase (HRP)-conjugated $F(ab')_2$ of anti-rabbit or mouse IgG (GE Healthcare) for 1 h at room temperature. The expression levels of these proteins were visualized using the ECL system (GE Healthcare) and an LAS3000 imager (Fujifilm).

2.5. LacZ gene activation and cytotoxicity of Cre-expressing AdVs

The Hep-CALNLZ cells were cultured on collagen-coated, 96-well plates and infected with AdVs at various MOIs in four-fold serial dilutions. After 48 h, cytotoxicity assays were performed using the Cell Counting Kit-8 (Dojindo Molecular Technologies), according to the manufacturer's instructions. To detect *LacZ* expression, the cells were fixed with 4% paraformaldehyde in PBS for 10 min, washed with PBS, and incubated in X-Gal solution (5 mM potassium ferricyanide, 5 mM potassium ferrocyanide, and 2 mM $MgCl_2$ in PBS) containing 0.5 mg/mL 5-bromo-4-chloro-3-indolyl-β-D-galactopyranoside (X-Gal; WAKO Pure Chemicals) at 37 °C overnight.

2.6. Extraction of total RNA and quantification of Ad-pIX mRNA levels

The HepG2 cells were infected with the AdVs at an MOI of 100 and were harvested after 24 h. The CN2-29 transgenic mice were injected with the AdVs at a dose of 1.0×10^9 PFU and were sacrificed to obtain their liver samples after 12 h. Total RNA was extracted from the cells or mouse livers using the RNeasy Mini Kit (Qiagen) and RNase-free DNase (Qiagen). Reverse transcription was performed using the High Capacity cDNA Reverse Transcription Kit (Applied Biosystems). Copy numbers of the Ad-pIX cDNA were assessed by quantitative real-time detection polymerase chain reaction (RTD-PCR) with the specific probe AdIX-354-S25FT (5′-[FAM]-TCAGCAGCTGTTGGATCTGCGCCAC-[TAMRA]-3′); AdIX-327-S24 (5′-TTTGACCCGGGAACTTAATGTCGT-3′) and AdIX-387-R19 (5′-GGAGGAAGCCTTCAGGGCA-3′) were used as primers. The standard curve was generated using pAxEFLacZ. Analyses were conducted using an ABI PRISM 7700 Sequence Detection System with TaqMan Universal PCR Master Mix (Applied Biosystems).

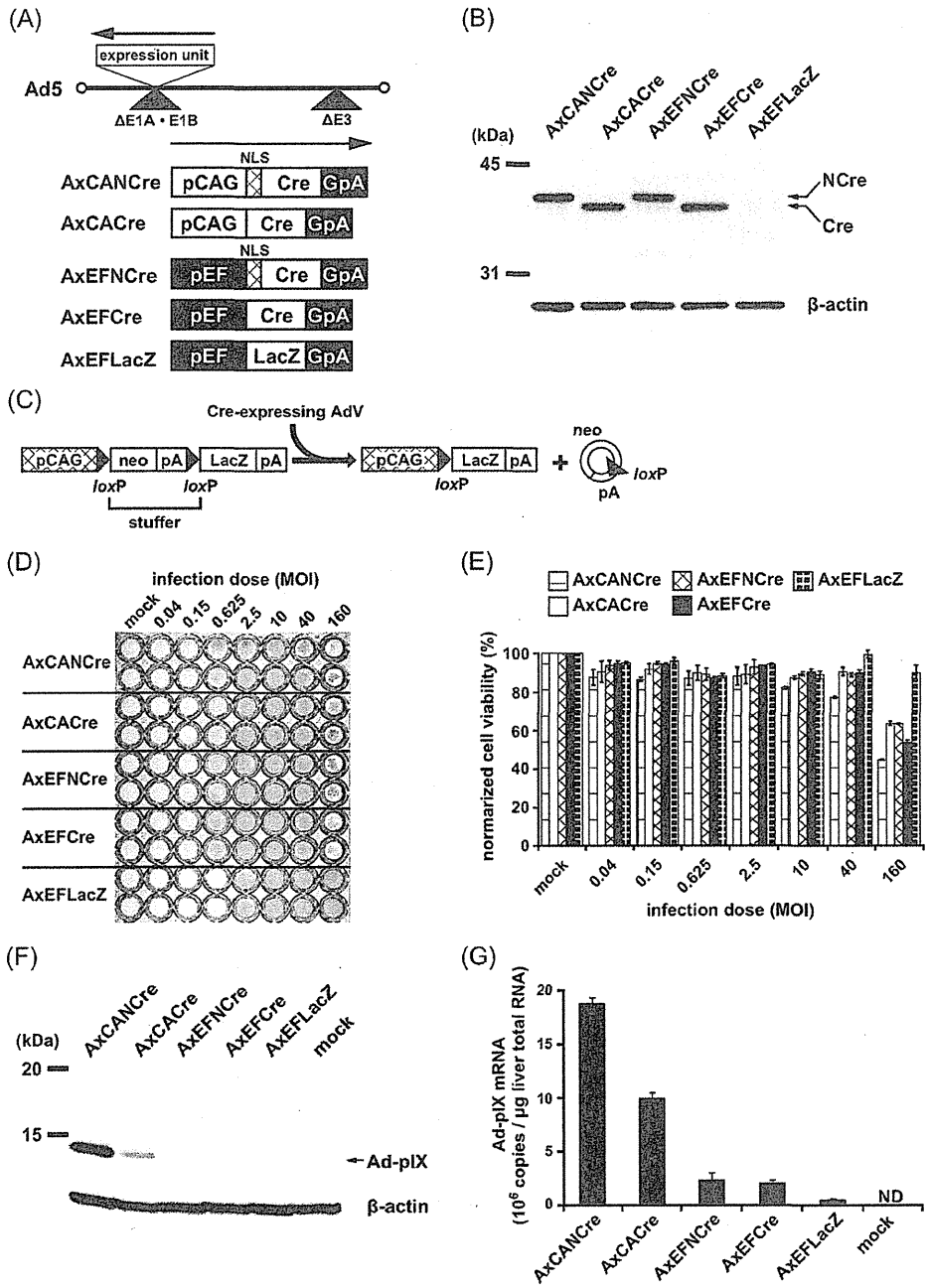

Fig. 1. Generation of AdVs expressing Cre under the control of different promoters. pCAG, CAG promoter; pEF, EF1α promoter; GpA, rabbit β-globin poly(A) signal; NLS, nuclear localization signal; neo, neomycin-resistance gene; pA, poly(A) signal; LacZ, β-galactosidase; Ad-pIX, adenovirus protein IX. (A) Structures of Cre-expressing AdVs. NLS-tagged Cre (NCre) or Cre were expressed under the control of the CAG or EF1α promoter. AxEFLacZ, which expresses LacZ under the control of the EF1α promoter, was used as a control. (B) Cre protein expression. HepG2 cells were infected with AdVs at an MOI of 20. After 24 h, total protein extracts from the cells were subjected to Western blotting. The detected β-actin protein is also shown. Note that mobility is slightly reduced when Cre is tagged with NLS (lanes, AxCANCre and AxEFNCre). (C) Schematic representation of *LacZ* transgene activation mediated by Cre-expressing AdV in Hep-CALNLZ cell chromosomes. Cre recognizes a pair of its target sequences *loxP* and removes the stuffer region as a circular DNA, resulting in expression of the transgene by the CAG promoter. (D) Cre recombination activity. Hep-CALNLZ cells were infected with Cre-expressing AdVs at the indicated dosages (four-fold serial dilutions; MOI range, 0.04–160). After 48 h, the cells were fixed and stained using X-gal staining. The first lane contains the mock-infected controls. The AxEFLacZ-infected lanes show the *LacZ*-gene-expressed control. (E) Cre cytotoxicities. Hep-CALNLZ cells were infected with AdVs at the indicated dosages (four-fold serial dilutions; MOI range, 0.04–160). After 48 h, cell viability was measured using a Cell Counting Kit-8. (F) Ad-pIX protein expression. HepG2 cells were infected with AdVs at an MOI of 100. After 24 h, total protein extracts from the cells were subjected to Western blotting. The detected β-actin protein is also shown. (G) mRNA expression of Ad-pIX. HepG2 cells were infected with AdVs at an MOI of 100. After 24 h, total RNA extracts from the cells were subjected to reverse transcription and quantitative RTD-PCR with an Ad-pIX-specific probe and a primer pair. ND, not detected.

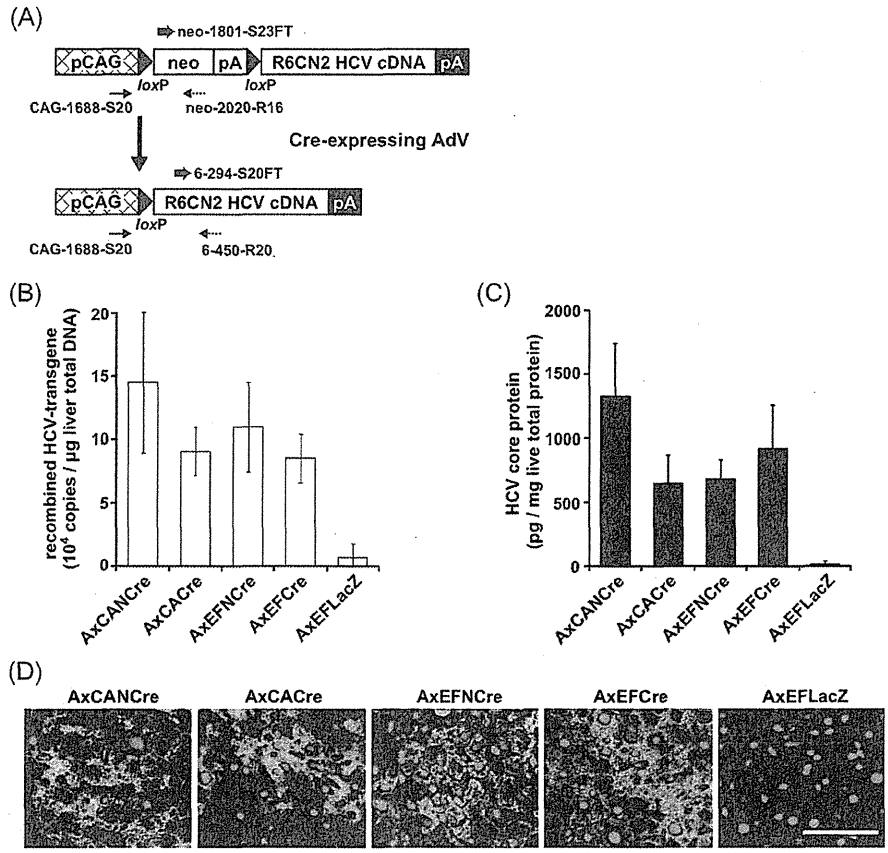

Fig. 2. Cre-mediated genomic DNA recombination and HCV core protein expression in transgenic mouse livers. (A) Structure of the Cre-mediated activation transgene unit CALNCN2 (Wakita et al., 1998). pCAG, CAG promoter; neo, neomycin-resistance gene; pA, poly(A) signal. The R6CN2 HCV cDNA (nucleotides 294–3435) contains the core, E1, E2, and NS2 regions. This construct does not allow HCV mRNA transcription prior to Cre-mediated DNA recombination, detected with the primer pair CAG-1688-S20 and neo-2020-R16. When Cre-expressing AdV is injected, the neo gene and poly(A) signal are removed by recombination between two *lox*P sequences. The recombined HCV transgene is detected with the primer pair CAG-1688-S20 and 6-450-R20. (B) Determination of Cre-mediated DNA recombination. CN2-29 transgenic mice were injected with 1.0×10^9 PFU for each AdV, and liver samples were harvested 7 days post-injection. Genomic DNA was extracted from the livers, and the numbers of copies of the recombined HCV-transgenes were determined using quantitative RTD-PCR with specific probes (6-294-S20FT) and a primer pair (CAG-1688-S20 and 6-450-R20). The values shown are means ± S.D. of more than three individual specimens. (C) Measurements of HCV core protein concentration in liver samples obtained from CN2-29 transgenic mice 7 days after injection of 1.0×10^9 PFU for each AdV. The samples were homogenized and the concentrations of HCV core protein were determined by EIA. The values shown are means ± S.D. of three individual specimens. (D) Immunofluorescence analysis of HCV core proteins. Liver sections of CN2-29 transgenic mice 7 days after injection of 1.0×10^9 PFU for each AdV were fixed and co-stained with rabbit anti-core polyclonal antibody (green) and DAPI (blue). Scale bar, 50 μm.

2.7. Determination of Cre-mediated HCV transgene recombination in mouse livers

The transgenic mouse livers were digested at 37 °C overnight in lysis buffer [50 mM Tris–HCl (pH 8.0), 0.1 M NaCl, 20 mM EDTA, 1% SDS] containing 1 mg/mL proteinase K. Total genomic DNA was then extracted using the phenol–chloroform extraction method. The copy numbers of the recombined HCV transgene in the livers were assessed via quantitative RTD-PCR (Takeuchi et al., 1999) with the specific probe 6-294-S20FT (5′-[FAM]-TGATAGGGTGCTTGCGAGTG-[TAMRA]-3′) and the primer pair CAG-1688-S20 (5′-GGTTGTTGTGCTGTCTCATC-3′) and 6-450-R20 (5′-ACAGGTAAACTCCACCAACG-3′) (Fig. 2A). The standard curve was generated using pCALNCN2/59-2 (Wakita et al., 1998) and quantitative RTD-PCR with the specific probe neo-1801-S23FT (5′-[FAM]-TCAAGAGACAGGATGAGGATCGT-[TAMRA]-3′) and the primer pair CAG-1688-S20 (5′-GGTTGTTGTGCTGTCTCATC-3′) and neo-2020-R16 (5′-TGCCTCGTCCTGCAGT-3′) (Fig. 2A). The *GAPDH* gene was used as an internal control for all samples. Analyses were carried out on an ABI PRISM 7700 Sequence Detection System with TaqMan Universal PCR Master Mix (Applied Biosystems).

2.8. Quantitation of HCV core proteins in mouse liver lysates

The transgenic mouse livers were homogenized in 0.5 mL RIPA buffer, and centrifuged at 15,000 rpm for 10 min at 4 °C. The protein concentrations of the supernatants were measured using the Bradford method (DC protein assay; Bio-Rad). The concentrations of HCV core proteins in the liver samples were determined using the Ortho HCV core protein ELISA kit (Eiken Chemical).

2.9. Biochemical analyses of mouse sera

Sequential blood samples were obtained by orbital bleeding after each AdV administration, and the sera were isolated by centrifugation at 10,000 rpm for 3 min at 4 °C. Serum ALT levels were determined using the Transaminase-CII Test A (Wako Pure Chemicals).

2.10. Histology and immunohistochemical staining

The liver samples were fixed with 4% paraformaldehyde in PBS, paraffin-embedded, sectioned at 4-μm thickness, and stained

with hematoxylin and eosin (H&E). Liver histology was evaluated according to modified Histology Activity Index (HAI) scores in three categories: piecemeal necrosis, spotty necrosis, and portal inflammation (Knodell et al., 1981; Yang et al., 1994).

The liver tissues were frozen in OCT compound (Tissue Tech) for immunohistochemical staining of HCV core proteins. The sections were fixed with a 1:1 solution of acetone:methanol at −20 °C for 10 min and then washed with PBS. Subsequently, the sections were incubated with the IgG fraction of an anti-HCV core rabbit polyclonal antibody (RR8) (Wakita et al., 1998) labeled with biotin in blocking buffer for 1 h at 4 °C. The sections were incubated with strept–avidin-conjugated horseradish peroxidase for 30 min at room temperature. Immunohistochemical staining was conducted using the Tyramide Signal Amplification Kit (Molecular Probes). Fluorescently labeled sections were stained with 4′,6-diamidino-2-phenylindole (DAPI; Molecular Probes) to stain the cell nuclei at room temperature before cover slipping. Fluorescence was observed under a fluorescence microscope (Carl Zeiss).

2.11. Statistical analysis

Data are shown as the mean ± S.D. Statistical analyses were performed using analysis of variance (ANOVA) followed by the Student–Newman–Keuls (SNK) test or analyzed using the unpaired Student's *t*-test. Statistical significance was established at $p < 0.05$.

3. Results

3.1. Generation of Cre-expressing AdVs

To enable HCV transgenic mice using the Cre/*lox*P system to express HCV protein persistently without severe inflammatory responses to AdV, we first constructed AdVs that expressed Cre with or without a nuclear localization signal (NLS) tag (AxEFNCre or AxEFCre, respectively) together with *LacZ* under the control of the EF1α promoter (AxEFLacZ) (Fig. 1A). AxCANCre and AxCACre were also generated to compare the impacts of using the CAG promoter and the EF1α promoter (Fig. 1A). Expression of Cre proteins from various AdVs was confirmed in human liver-derived HepG2 cells by Western blot analysis (Fig. 1B). Cre protein expression levels were not significantly different whether the gene was expressed under the control of the CAG or the EF1α promoter in the HepG2 cells (Fig. 1B). Next, we examined the recombination activities of Cre expressed via the AdVs using the Hep-CALNLZ cell line, HepG2 cells that express CALNLZ (Fig. 1C). When the Cre-expressing AdVs bearing the CAG or EF1α promoters infected these cells, the blue color produced by *LacZ* activation was observed for MOIs of 0.15–160. The cells infected with AxEFLacZ showed the blue staining in an MOI-dependent manner (Fig. 1D, lane AxEFLacZ). In contrast, the color faded for MOIs >40 when the Cre-expressing AdVs were used (Fig. 1D, lanes AxCANCre, AxCACre, AxEFNCre, and AxEFCre). At an MOI of 160, all of the Cre-expressing AdVs resulted in cytotoxicity, while the LacZ-expressing AdV did not affect cell viability (Fig. 1E).

AdV-induced immune responses are partly caused by co-expression of Ad-pIX (Nakai et al., 2007). To confirm the protein expression levels of Ad-pIX due to the AdVs, we performed Western blotting with anti-Ad-pIX sera (Fig. 1F). When HepG2 cells were infected with AdVs bearing the CAG promoter, significant amounts of Ad-pIX were detected as 14-kDa bands (Fig. 1F, lanes AxCANCre and AxCACre). In contrast, when using AdVs bearing the EF1α promoter, the 14-kDa band representing Ad-pIX was undetectable, as was the case for mock-infected HepG2 cells (Fig. 1F, lanes AxEFNCre, AxEFCre, AxEFLacZ, and mock). We also examined the mRNA expression levels of Ad-pIX and obtained similar results that correlated with the protein expression levels (Fig. 1G).

3.2. HCV gene expression and core protein production mediated by various Cre-expressing AdVs in transgenic mouse livers

The HCV transgenic mouse CN2-29 contains a reporter unit (CALNCN2) that is activated by Cre and conditionally expresses the HCV gene (Fig. 2A; Wakita et al., 1998). To assess the efficiency of Cre-expressing AdVs in promoting HCV gene expression, we intravenously injected the CN2-29 transgenic mice with various AdVs. At 7 days post-injection, Cre protein expression was confirmed by Western blot analysis of liver lysates (data not shown). The recombined HCV transgene levels in the livers were determined by quantitative RTD-PCR using specific probes and primer pairs, as described in Section 2 (Fig. 2A and B). When each Cre-expressing AdV was injected, the respective recombined HCV transgene was detectable; AxCANCre-injected CN2-29 transgenic mice expressed the highest levels of the recombined HCV transgene in their livers (Fig. 2B). CN2-29 transgenic mice injected with AdVs expressing NLS-tagged Cre had higher levels of the recombined HCV transgene in their livers (Fig. 2B, AxCANCre and AxEFNCre). This result suggests that NLS-tagged Cre efficiently translocated to the cell nucleus, which is consistent with our previous data (Baba et al., 2005). However, the levels of the recombined HCV transgene were not correlated with the expression level of HCV core protein (Fig. 2C).

The core protein levels in the livers were measured by enzyme immunoassay (EIA) as described in Section 2. The expression of the E1 and E2 proteins in the CN2–29 transgenic mouse livers has been shown previously (Wakita et al., 1998). The mean core protein level was 1.3 ng/mg total protein in the CN2-29 transgenic mouse livers 7 days after administration of AxCANCre (Fig. 2C). AxCACre- and AxEFNCre-injected mice expressed approximately one-half of the core protein levels resulting from AxCANCre injection (Fig. 2C).

Expression of core proteins in AdV-injected CN2-29 transgenic mouse livers was confirmed through immunofluorescence staining. Core proteins were expressed in the hepatocytes in the lobules of liver sections from Cre-expressing AdV-injected mice (Fig. 2D). In contrast, AxEFLacZ-injected transgenic mice did not express core proteins (Fig. 2C and D).

3.3. Liver injury and Ad-pIX expression in HCV transgenic mice injected with AdVs

To evaluate hepatocellular injury caused by expression of HCV proteins in CN2-29 transgenic mice injected with Cre-expressing AdVs, we serially estimated the serum ALT levels (Fig. 3A). For AxCANCre, the serum ALT level was elevated on day 5 and peaked 1–2 weeks post-injection (Fig. 3A, open triangle). ALT levels in AxCACre-injected transgenic mice were also elevated, although these levels declined over time (Fig. 3A, open circle). When AxEFNCre or AxEFCre was injected, ALT levels did not immediately increase, although they gradually increased after day 5 (Fig. 3A, closed triangle and closed circle, respectively). Injection of AxEFLacZ did not increase serum ALT levels in the CN2-29 transgenic mice (Fig. 3A, closed rectangle).

We also performed histological analyses of liver sections from CN2–29 transgenic mice 7 days after AdV injection (Fig. 3B). We found that severe inflammation with lymphocyte infiltration and spotty necrosis were diffusely observed in the livers of mice injected with the AdVs bearing the CAG promoter (AxCACre and AxCANCre) (Fig. 3B, a,b). In contrast, AxEFNCre-injected and AxEFCre-injected transgenic mouse livers exhibited mild inflammation without massive piecemeal necrosis on day 7 (Fig. 3B, c,d). No inflammation was observed in the AxEFLacZ-injected mice (Fig. 3B, e).

To confirm the expression levels of Ad-pIX in AdV-injected transgenic mice, we determined Ad-pIX mRNA in the liver using

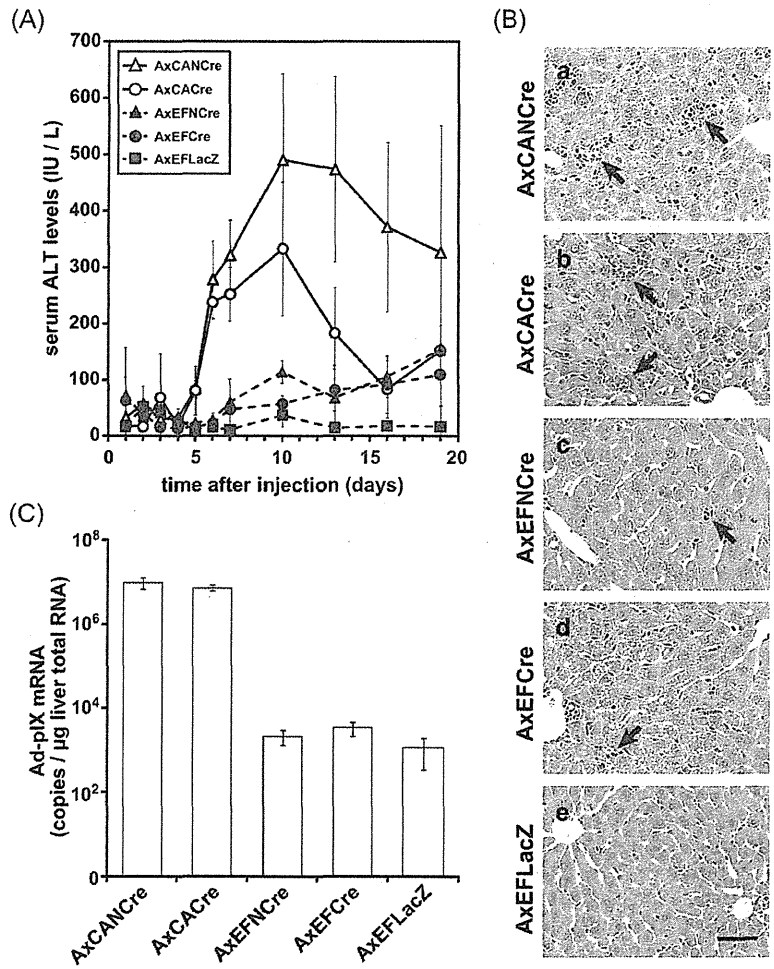

Fig. 3. Effects of AdVs on liver injuries in HCV transgenic mice. (A) Serum ALT levels were measured at the indicated time-points in CN2-29 transgenic mice injected with 1.0×10^9 PFU AxCANCre (open triangle), AxCACre (open circle), AxEFNCre (closed triangle), AxEFCre (closed circle), and AxEFLacZ (closed rectangle). The ALT levels are shown as means ± S.D. of three individual specimens. (B) Histopathologic changes in the livers of transgenic mice 7 days after injection of each AdV. The liver sections were stained with H&E. The arrows represent lymphocyte infiltrations. Scale bar, 50 μm. (C) mRNA expression of Ad-pIX in the livers. CN2-29 transgenic mice were injected with 1.0×10^9 PFU of the AdVs. After 12 h, the livers were harvested. The total RNA extracts from the livers were subjected to reverse transcription and RTD-PCR with an Ad-pIX-specific probe and a primer pair, as described in Section 2. The numbers of copies of Ad-pIX mRNA are shown as means ± S.D. of three individual specimens.

reverse transcription and quantitative RTD-PCR, as described under Section 2. The copy numbers of Ad-pIX mRNA were quite high in transgenic mice that were injected with AdV bearing the CAG promoter (Fig. 3C). The observed inflammation levels were consistent with the expression levels of Ad-pIX.

3.4. Liver inflammatory responses to the HCV protein inducibly expressed by AdVs in transgenic mice

Because our results indicated that severe liver injuries were caused by AdVs bearing the CAG promoter, we evaluated liver inflammatory responses to the HCV protein inducibly expressed by AdVs in transgenic mice 7 days post-injection according to the modified HAI scoring system (Fig. 4A) (Knodell et al., 1981; Yang et al., 1994). Among the transgenic mice, more severe liver damage was observed in those that were injected with Cre-expressing AdVs bearing the CAG promoter (Fig. 4A, AxCANCre and AxCACre) compared to those injected with Cre-expressing AdVs bearing the EF1α promoter (Fig. 4A, AxEFNCre and AxEFCre).

Because AxEFCre more efficiently expressed HCV proteins than AxEFNCre (Fig. 2C and D), we injected AxEFCre into transgenic mice and wild-type mice to examine the effects of HCV protein expression. The severity of liver inflammation in the AxEFCre-injected transgenic mice was significantly greater than in the AxEFCre-injected wild-type mice or the AxEFLacZ-injected transgenic mice (Fig. 4A and B).

Seven days after AdV administration, serum ALT levels of AxCANCre-injected wild-type mice were significantly higher than those of AxEFCre-injected wild-type mice (Fig. 4C). This ALT elevation was observed in both transgenic and wild-type mice injected with AxCANCre (Fig. 4C). In contrast, AxEFCre was injected into the two groups, transgenic mice expressing HCV proteins exhibited more severe liver injury than wild-type mice (Fig. 4C and D).

3.5. Effects of Cre-expressing AdV bearing the EF1α promoter on HCV protein expression in transgenic mouse livers

To investigate whether CN2-29 transgenic mice injected with AdVs bearing the EF1α promoter showed liver inflammation caused

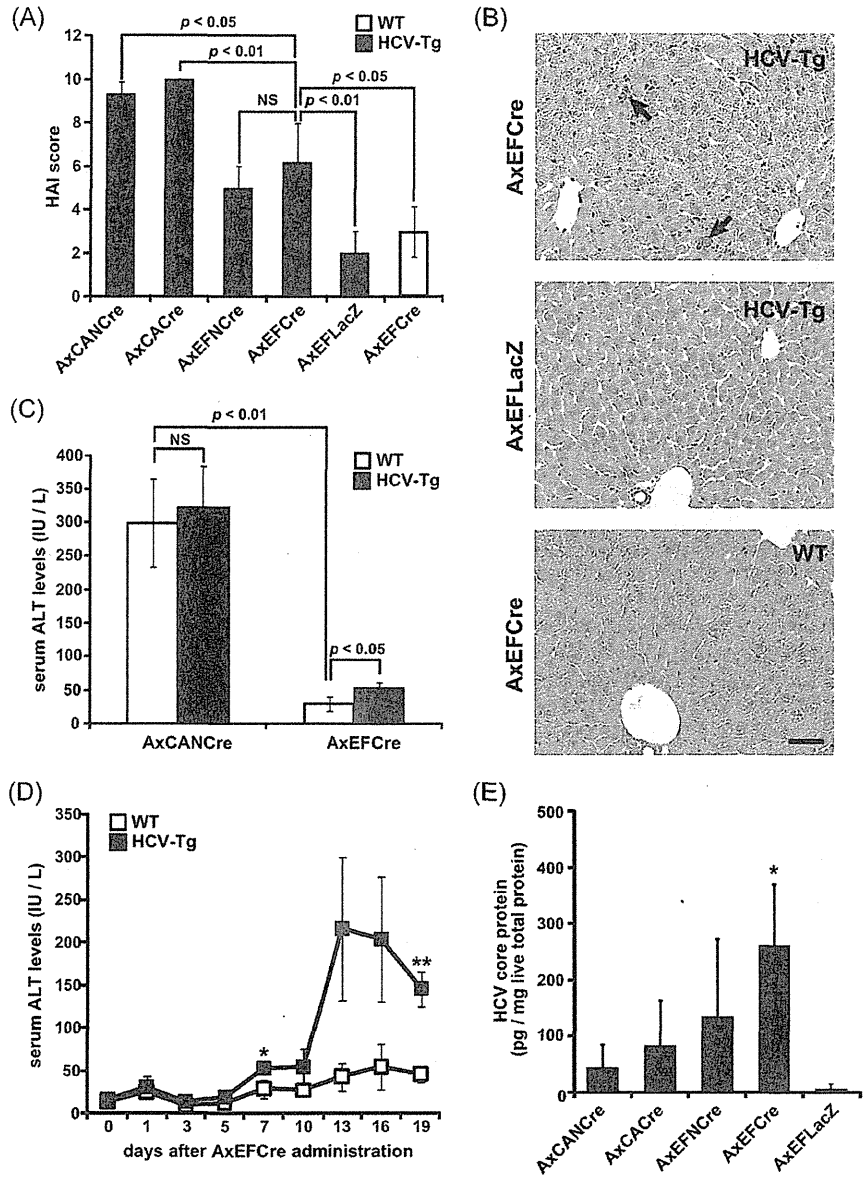

Fig. 4. Liver inflammatory responses due to HCV protein expression induced by AxEFCre. (A) Histopathology of mouse livers after injection of AdVs. Histopathologic features of the livers of CN2-29 transgenic mice (HCV-Tg, closed bars) injected with 1.0×10^9 PFU of AxCANCre, AxCACre, AxEFNCre, AxEFCre, or AxEFLacZ, and wild-type mice that were injected with 1.0×10^9 PFU of AxEFCre at day 7 post-injection (WT, opened bar). Pathologic changes were evaluated by light microscopy of H&E-stained sections of the mouse livers using the modified HAI scoring system. The extent of pathology was scored on a scale from 0 (none) to 12 (severe). All of the scores are means ± S.D. of more than three individual specimens. Statistical analysis was performed using an unpaired Student's *t*-test. NS, not significant. (B) Histopathologic changes resulting from HCV protein expression in mouse livers. CN2-29 transgenic mice (HCV-Tg) were injected with AxEFCre or AxEFLacZ and wild-type mice (WT) were injected with AxEFCre 7 days post-injection. The liver sections were stained with H&E. The arrows represent piecemeal necrosis. Scale bars, 50 μm. (C) Serum ALT levels with or without HCV protein expression 7 days after administration of the AdVs. Statistical analysis was performed using an unpaired Student's *t*-test between CN2-29 transgenic mice (HCV-Tg) and wild-type mice (WT). NS, not significant. (D) Sequential changes in serum ALT levels after AxEFCre administration. Serum ALT levels were measured at the indicated time-points in CN2-29 transgenic mice (HCV-Tg, closed square) or wild-type mice (WT, opened square) that were injected with 1.0×10^9 PFU AxEFCre. ALT levels are shown as means ± S.D. of more than three individual specimens. Statistical analysis was performed using an unpaired Student's *t*-test between CN2-29 transgenic mice (HCV-Tg) and wild-type mice (WT). $^*p < 0.05$; $^{**}p < 0.01$. (E) HCV core protein expression 21 days after AdV administration in transgenic mouse livers. CN2-29 transgenic mice were injected with 1.0×10^9 PFU for each AdV. After 21 days, the livers were harvested and homogenized. The concentrations of HCV core proteins in liver lysates were determined by EIA. The values shown are means ± S.D. of three individual experiments. Statistical analysis was performed using an ANOVA, followed by the SNK test. $^*p < 0.05$.

by persistently expressed HCV proteins, we evaluated core proteins by EIA in transgenic mouse livers 21 days post-injection of the AdVs (Fig. 4E). HCV core protein expression was scarcely detectable in the transgenic mice injected with AxCANCre, while the AxEFCre-injected transgenic mice showed significantly higher levels of core protein expression (Fig. 4E). Although, the AxCANCre injection was scarcely observed at day 21 in the transgenic mice (Fig. 4E), HCV core protein expression induced by AxEFCre injection was observed until at least day 56.

4. Discussion

In the present study, we demonstrated that Cre-expressing AdVs bearing the EF1α promoter induce HCV gene expression and

HCV protein production without induction of severe liver injury in inducible-HCV transgenic mice. We further observed that increases in serum ALT levels and liver inflammation were related to HCV protein expression mediated by AxEFCre injection. Moreover, AxEFCre injection enabled the transgenic mice to persistently express HCV proteins.

In previous studies, HCV transgenic mice constitutively expressing HCV proteins exhibited symptoms of steatosis and/or hepatocellular carcinoma, but did not show inflammatory or immunopathologic changes (Lerat et al., 2002; Moriya et al., 1997, 1998; Sun et al., 2001). Inducible-HCV transgenic mouse lineages, in which HCV protein expression is regulated, have enabled investigation of the immunopathogenesis of HCV protein expression. HCV transgenic mice regulated by the Cre/*lox*P system (Sun et al., 2005; Tumurbaatar et al., 2007; Wakita et al., 1998) or the tetracycline regulatory system (Ernst et al., 2007) exhibit inducible and liver-specific expression of HCV proteins. Inducible-HCV transgenic mice using the Cre/*lox*P system with an AdV that expresses Cre under the control of the CAG promoter (AxCANCre) exhibit HCV-specific immune responses (Wakita et al., 1998, 2000). The inducible-HCV CN2-29 transgenic mice, which express the core, E1, E2, and NS2 proteins, have HCV-specific cytotoxic T lymphocytes (Takaku et al., 2003; Wakita et al., 1998, 2000).

However, they show severe inflammatory responses to AxCANCre itself and thus, HCV protein expression is only transient (Wakita et al., 2000). These significant obstacles have limited the utility of inducible-HCV transgenic mice. Therefore, to deliver the *Cre* gene into the liver, non-adenoviral induction methods have been developed (Ho et al., 2008; Sun et al., 2005; Zhu et al., 2006). Meanwhile, adenoviral genes that cause cellular immune responses have been identified and modified AdVs that do not trigger host immune responses have been developed (Palmer and Ng, 2005). A recent study demonstrated that immune responses to AdVs bearing the CAG promoter were associated with co-expression of Ad-pIX, whereas immune responses were minimal when transgene expression was controlled by the EF1α promoter (Nakai et al., 2007). Therefore, we postulated that severe inflammation of mouse livers after administration of Cre-expressing AdVs bearing the CAG promoter (AxCANCre) might be caused by expression of Ad-pIX. In the present study, we generated Cre-expressing AdVs bearing the EF1α promoter (AxEFCre) and infected HCV transgenic mice. AxEFCre-injected mice expressed much less Ad-pIX mRNA and did not show the increased levels of ALT or severe liver inflammation as did Cre-expressing AdVs under the control of the CAG promoter (Fig. 3). In contrast, AxCANCre administration caused severe liver injury in both HCV transgenic mice and wild-type mice (Fig. 4D; Wakita et al., 2000). AxEFCre administration caused liver injury in the HCV transgenic mice, but not in the wild-type mice (Fig. 4A–D). These results suggest that AxEFCre alone induces only minimal host immune responses compared to AxCANCre; therefore, the liver inflammatory responses exhibited by AxEFCre-injected transgenic mice were clearly due to expression of HCV proteins. Because AxCANCre injection alone causes severe liver injuries, most of the hepatocytes infected with AxCANCre are eliminated and HCV protein expression in the livers of transgenic mice is only transient (Wakita et al., 2000). On the other hand, AxEFCre injection did not induce such severe liver injuries. The AxEFCre-injected HCV transgenic mice showed milder liver inflammation in response to expression of HCV proteins and persistently expressed HCV proteins without elimination of hepatocytes infected with AxEFCre.

In conclusion, HCV gene expression mediated by the Cre/*lox*P system and a Cre-expressing AdV that bears the EF1α promoter, AxEFCre, enables Cre-mediated recombination of transgenes in mice without inducing severe liver injury due to the AdV itself. Moreover, this inducible-HCV transgenic mouse model should be useful for investigation of liver injury due to HCV and the pathogenesis of HCV.

Acknowledgments

The authors wish to thank Mitsugu Takahashi for breeding the transgenic mice. This study was supported by grants from the Ministry of Education, Culture, Sports, Science and Technology of Japan; the Program for Promotion of Fundamental Studies in Health Sciences of the Pharmaceuticals and Medical Devices Agency of Japan; and the Ministry of Health, Labor and Welfare of Japan.

References

Akagi, K., Sandig, V., Vooijs, M., Van der Valk, M., Giovannini, M., Strauss, M., Berns, A., 1997. Cre-mediated somatic site-specific recombination in mice. Nucleic Acids Res. 25 (9), 1766–1773.

Baba, Y., Nakano, M., Yamada, Y., Saito, I., Kanegae, Y., 2005. Practical range of effective dose for Cre recombinase-expressing recombinant adenovirus without cell toxicity in mammalian cells. Microbiol. Immunol. 49 (6), 559–570.

Bangari, D.S., Mittal, S.K., 2006. Current strategies and future directions for eluding adenoviral vector immunity. Curr. Gene Ther. 6 (2), 215–226.

Ernst, E., Schonig, K., Bugert, J.J., Blaker, H., Pfaff, E., Stremmel, W., Encke, J., 2007. Generation of inducible hepatitis C virus transgenic mouse lines. J. Med. Virol. 79 (8), 1103–1112.

Goodman, Z.D., Ishak, K.G., 1995. Histopathology of hepatitis C virus infection. Semin. Liver Dis. 15 (1), 70–81.

Ho, K.J., Bass, C.E., Kroemer, A.H., Ma, C., Terwilliger, E., Karp, S.J., 2008. Optimized adeno-associated virus 8 produces hepatocyte-specific Cre-mediated recombination without toxicity or affecting liver regeneration. Am. J. Physiol. Gastrointest. Liver Physiol. 295 (2), G412–G419.

Kafri, T., Morgan, D., Krahl, T., Sarvetnick, N., Sherman, L., Verma, I., 1998. Cellular immune response to adenoviral vector infected cells does not require de novo viral gene expression: implications for gene therapy. Proc. Natl. Acad. Sci. U S A 95 (19), 11377–11382.

Kanegae, Y., Lee, G., Sato, Y., Tanaka, M., Nakai, M., Sakaki, T., Sugano, S., Saito, I., 1995. Efficient gene activation in mammalian cells by using recombinant adenovirus expressing site-specific Cre recombinase. Nucleic Acids Res. 23 (19), 3816–3821.

Kanegae, Y., Makimura, M., Saito, I., 1994. A simple and efficient method for purification of infectious recombinant adenovirus. Jpn. J. Med. Sci. Biol. 47 (3), 157–166.

Knodell, R.G., Ishak, K.G., Black, W.C., Chen, T.S., Craig, R., Kaplowitz, N., Kiernan, T.W., Wollman, J., 1981. Formulation and application of a numerical scoring system for assessing histological activity in asymptomatic chronic active hepatitis. Hepatology 1 (5), 431–435.

Kobayashi, N., Fujiwara, T., Westerman, K.A., Inoue, Y., Sakaguchi, M., Noguchi, H., Miyazaki, M., Cai, J., Tanaka, N., Fox, I.J., Leboulch, P., 2000. Prevention of acute liver failure in rats with reversibly immortalized human hepatocytes. Science 287 (5456), 1258–1262.

Kremsdorf, D., Brezillon, N., 2007. New animal models for hepatitis C viral infection and pathogenesis studies. World J. Gastroenterol. 13 (17), 2427–2435.

Lerat, H., Honda, M., Beard, M.R., Loesch, K., Sun, J., Yang, Y., Okuda, M., Gosert, R., Xiao, S.Y., Weinman, S.A., Lemon, S.M., 2002. Steatosis and liver cancer in transgenic mice expressing the structural and nonstructural proteins of hepatitis C virus. Gastroenterology 122 (2), 352–365.

Moriya, K., Fujie, H., Shintani, Y., Yotsuyanagi, H., Tsutsumi, T., Ishibashi, K., Matsuura, Y., Kimura, S., Miyamura, T., Koike, K., 1998. The core protein of hepatitis C virus induces hepatocellular carcinoma in transgenic mice. Nat. Med. 4 (9), 1065–1067.

Moriya, K., Yotsuyanagi, H., Shintani, Y., Fujie, H., Ishibashi, K., Matsuura, Y., Miyamura, T., Koike, K., 1997. Hepatitis C virus core protein induces hepatic steatosis in transgenic mice. J. Gen. Virol. 78 (7), 1527–1531.

Nakai, M., Komiya, K., Murata, M., Kimura, T., Kanaoka, M., Kanegae, Y., Saito, I., 2007. Expression of pIX gene induced by transgene promoter: possible cause of host immune response in first-generation adenoviral vectors. Hum. Gene. Ther. 18 (10), 925–936.

Palmer, D.J., Ng, P., 2005. Helper-dependent adenoviral vectors for gene therapy. Hum. Gene. Ther. 16 (1), 1–16.

Shepard, C.W., Finelli, L., Alter, M.J., 2005. Global epidemiology of hepatitis C virus infection. Lancet Infect. Dis. 5 (9), 558–567.

Shintani, Y., Yotsuyanagi, H., Moriya, K., Fujie, H., Tsutsumi, T., Kanegae, Y., Kimura, S., Saito, I., Koike, K., 1999. Induction of apoptosis after switch-on of the hepatitis B virus X gene mediated by the Cre/loxP recombination system. J. Gen. Virol. 80 (12), 3257–3265.

Sun, J., Bodola, F., Fan, X., Irshad, H., Soong, L., Lemon, S.M., Chan, T.S., 2001. Hepatitis C virus core and envelope proteins do not suppress the host's ability to clear a hepatic viral infection. J. Virol. 75 (24), 11992–11998.

Sun, J., Tumurbaatar, B., Jia, J., Diao, H., Bodola, F., Lemon, S.M., Tang, W., Bowen, D.G., McCaughan, G.W., Bertolino, P., Chan, T.S., 2005. Parenchymal expression of CD86/B7.2 contributes to hepatitis C virus-related liver injury. J. Virol. 79 (16), 10730–10739.

Takaku, S., Nakagawa, Y., Shimizu, M., Norose, Y., Maruyama, I., Wakita, T., Takano, T., Kohara, M., Takahashi, H., 2003. Induction of hepatic injury by hepatitis C-virus-

specific CD8± murine cytotoxic T lymphocytes in transgenic mice expressing the viral structural genes. Biochem. Biophys. Res. Commun. 301, 330–337.
Takeuchi, T., Katsume, A., Tanaka, T., Abe, A., Inoue, K., Tsukiyama-Kohara, K., Kawaguchi, R., Tanaka, S., Kohara, M., 1999. Real-time detection system for quantification of hepatitis C virus genome. Gastroenterology 116 (3), 636–642.
Tumurbaatar, B., Sun, Y., Chan, T., Sun, J., 2007. Cre-estrogen receptor-mediated hepatitis C virus structural protein expression in mice. J. Virol. Methods 146 (1–2), 5–13.
Wakita, T., Katsume, A., Kato, J., Taya, C., Yonekawa, H., Kanegae, Y., Saito, I., Hayashi, Y., Koike, M., Miyamoto, M., Hiasa, Y., Kohara, M., 2000. Possible role of cytotoxic T cells in acute liver injury in hepatitis C virus cDNA transgenic mice mediated by Cre/loxP system. J. Med. Virol. 62 (3), 308–317.
Wakita, T., Taya, C., Katsume, A., Kato, J., Yonekawa, H., Kanegae, Y., Saito, I., Hayashi, Y., Koike, M., Kohara, M., 1998. Efficient conditional transgene expression in hepatitis C virus cDNA transgenic mice mediated by the Cre/loxP system. J. Biol. Chem. 273 (15), 9001–9006.
Yang, Y., Ertl, H.C., Wilson, J.M., 1994. MHC class I-restricted cytotoxic T lymphocytes to viral antigens destroy hepatocytes in mice infected with E1-deleted recombinant adenoviruses. Immunity 1 (5), 433–442.
Zhu, H.Z., Wang, W., Feng, D.M., Sai, Y., Xue, J.L., 2006. Conditional gene modification in mouse liver using hydrodynamic delivery of plasmid DNA encoding Cre recombinase. FEBS Lett. 580 (18), 4346–4352.

UNC93B1 Physically Associates with Human TLR8 and Regulates TLR8-Mediated Signaling

Hiroki Itoh[9], Megumi Tatematsu[9], Ayako Watanabe[9¤], Katsunori Iwano, Kenji Funami, Tsukasa Seya, Misako Matsumoto*

Department of Microbiology and Immunology, Hokkaido University Graduate School of Medicine, Sapporo, Japan

Abstract

Toll-like receptors (TLRs) 3, 7, 8, and 9 are localized to intracellular compartments where they encounter foreign or self nucleic acids and activate innate and adaptive immune responses. The endoplasmic reticulum (ER)-resident membrane protein, UNC93B1, is essential for intracellular trafficking and endolysosomal targeting of TLR7 and TLR9. TLR8 is phylogenetically and structurally related to TLR7 and TLR9, but little is known about its localization or function. In this study, we demonstrate that TLR8 localized to the early endosome and the ER but not to the late endosome or lysosome in human monocytes and HeLa transfectants. UNC93B1 physically associated with human TLR8, similar to TLRs 3, 7, and 9, and played a critical role in TLR8-mediated signaling. Localization analyses of TLR8 tail-truncated mutants revealed that the transmembrane domain and the Toll/interleukin-1 receptor domain were required for proper targeting of TLR8 to the early endosome. Hence, although UNC93B1 participates in intracellular trafficking and signaling for all nucleotide-sensing TLRs, the mode of regulation of TLR localization differs for each TLR.

Citation: Itoh H, Tatematsu M, Watanabe A, Iwano K, Funami K, et al. (2011) UNC93B1 Physically Associates with Human TLR8 and Regulates TLR8-Mediated Signaling. PLoS ONE 6(12): e28500. doi:10.1371/journal.pone.0028500

Editor: Nick Gay, University of Cambridge, United Kingdom

Received August 3, 2011; **Accepted** November 9, 2011; **Published** December 2, 2011

Funding: This work was supported in part by Grants-in-Aid from the Ministry of Education, Science, and Culture, the Ministry of Health, Labor, and Welfare of Japan, and by the Akiyama Life Science Foundation. The funders had no role in study design, data collection and analysis, decision to publish, or preparation of the manuscript.

Competing Interests: The authors have declared that no competing interests exist.

* E-mail: matumoto@pop.med.hokudai.ac.jp

[9] These authors contributed equally to this work.

¤ Current address: Department of Cancer Biology, The Institute of Medical Science, The University of Tokyo, Tokyo, Japan

Introduction

The innate immune system discriminates self from non-self by expressing germ-line encoded receptors that recognize pathogen- or damage-associated molecular patterns [1-3]. The Toll-like receptor (TLR) family of type I transmembrane proteins were the first group of pattern recognition receptors to be identified [4]. Within this family, TLRs 3, 7, 8, and 9 recognize microbial nucleic acids and induce cytokine production, including type I interferon (IFN), and dendritic cell (DC) maturation [2]. In humans, TLR7 and TLR9 are selectively expressed in B cells and plasmacytoid DCs, while TLR3 and TLR8 are expressed in myeloid DCs [5–8].

TLR8 is phylogenetically and structurally related to TLR7 [9,10]; they both recognize ssRNA and an imidazoquinoline compound [11–13]. In mice, TLR8 appears to be nonfunctional in most tissues and cells, except for the brain [14,15]. Human TLR8 is expressed in myeloid cells, such as monocytes, macrophages, and myeloid DCs, and also, in regulatory T cells [6,16,17]. Upon stimulation with synthetic ligands, human TLR8 activates NF-κB via the adaptor protein MyD88, which leads to the induction of proinflammatory cytokines but, not type I IFN [13]. In contrast, human/mouse TLR7 strongly induces type I IFN production in response to ssRNA and an imidazoquinoline compound. The differential expression and cytokine profiles of human TLR8 compared with those of human/mouse TLR7 suggest that human TLR8 plays a distinct role in the anti-viral immune response.

Notably, these nucleotide-sensing TLRs are localized to intracellular compartments. Human TLR3 localizes to the early endosome where it recognizes exogenous dsRNA and generates signals via Toll/interleukin-1 receptor (TIR)-containing adaptor molecule-1 (TICAM-1), also named TIR domain-containing adaptor-inducing IFN-β [8,18–20]. A linker region between the transmembrane domain and the TIR domain consisting of 26 amino acids determines the subcellular localization of human TLR3 [21]. In contrast, the transmembrane domain is the main determinant for intracellular localization of mouse TLR7 and TLR9 [22,23]. The endoplasmic reticulum (ER)-resident membrane protein, UNC93B1, physically associates with TLR7 and TLR9 and delivers them to endolysosomes [24,25]. After the trafficking of TLR7 and TLR9 from the ER to the endolysosome, their ectodomains are cleaved to generate a functional receptor [26,27]. UNC93B1 also interacts with TLR3 [24], but its role in the intracellular trafficking of TLR3 remains undefined; however, the interaction of UNC93B1 with the TLR3, 7, and 9 transmembrane regions is essential for the signaling function of these TLRs [28,29]. In contrast, there is little information concerning the subcellular localization and trafficking of human TLR8.

In this study, we analyzed the subcellular localization of TLR8 in human monocytes and HeLa transfectants and demonstrated that TLR8 was localized to the early endosome and the ER but not to the late endosome or lysosome. Using a series of TLR8

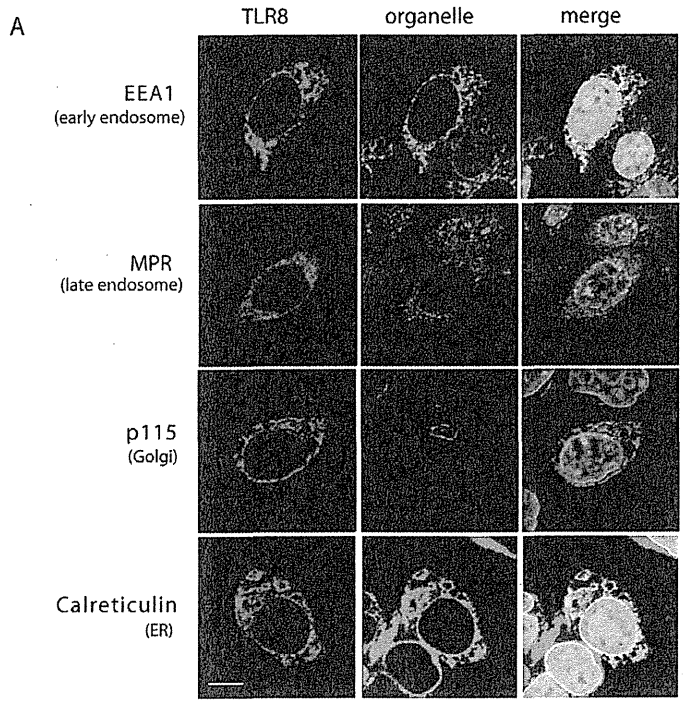
A
TLR8
organelle
merge
EEA1
(early endosome)
MPR
(late endosome)
p115
(Golgi)
Calreticulin
(ER)

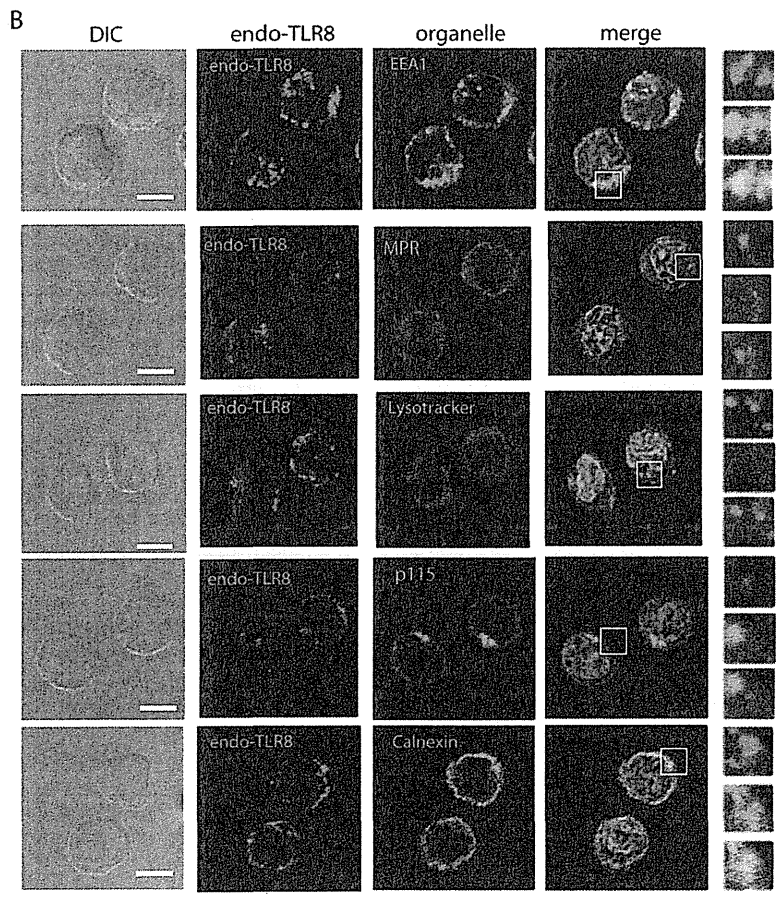
B
DIC
endo-TLR8
organelle
merge
endo-TLR8
EEA1
endo-TLR8
MPR
endo-TLR8
Lysotracker
endo-TLR8
p115
endo-TLR8
Calnexin

Figure 1. Subcellular localization of TLR8 in human monocytes and HeLa transfectants. HeLa cells transiently expressing human TLR8 (*A*) and human monocytes (*B*) were incubated with anti-FLAG mAb (*A*) or anti-TLR8 mAb (*B*) followed by an Alexa Fluor 488-conjugated secondary Ab. Organelles were stained with an anti-EEA1 pAb, anti-MPR pAb, anti-p115 pAb, anti-calreticulin pAb, or anti-calnexin pAb followed by an Alexa Fluor 568-conjugated secondary Ab. Representative confocal images are shown. Green, TLR8; red, organelle markers; blue, nuclei stained with DAPI. Scale bar: (*A*) 10 μm; (*B*) 5 μm.
doi:10.1371/journal.pone.0028500.g001

deletion mutants, we demonstrated that both the transmembrane and the TIR domains are required for the intracellular localization of TLR8. Furthermore, we showed that UNC93B1 physically associates with TLR8 and regulates TLR8-mediated signaling.

Results

Human TLR8 localizes to the early endosome and the ER in human monocytes

Intracellular expression of TLR8 was first analyzed using a chimeric receptor composed of the extracellular domain of murine TLR4 fused with the transmembrane and cytoplasmic regions of murine TLR8 [22]. Subsequently, intact human TLR8 was shown to localize intracellularly in transfected cells [30]. However, the site of localization of TLR8 remained unknown. We therefore analyzed the subcellular localization of human TLR8 in HeLa cells transiently expressing FLAG-tagged human TLR8. When examined using confocal microscopy, TLR8-positive compartments colocalized with the early endosome antigen 1 (EEA1) and the ER marker calreticulin (Fig. 1A). Late endosome (MPR), lysosome (LAMP-1), and Golgi (p115) markers did not colocalize with TLR8 (Fig. 1A and data not shown). TLR8 is expressed in human monocytes and induces the cytokine production in response to a synthetic TLR8 ligand [13]; therefore, we next examined the subcellular localization of endogenous TLR8 in human monocytes. TLR8 was localized to the early endosome and the ER but not to the late endosome/lysosome or Golgi (Fig. 1B). Thus, the localization site of TLR8 differed from TLR7 and TLR9, both of which reside in the endolysosome and the ER.

The TIR domain is required for endosomal localization of human TLR8

To determine which region is responsible for the intracellular localization and trafficking of human TLR8, we constructed tail-truncated mutants (Fig. 2A). These included a mutant lacking the TIR domain but retaining the proximal 31 amino acids (delTIR, 1–896 a.a.), one that lacked the cytoplasmic tail (delCYT, 1–866 a.a.), and a mutant lacking the transmembrane domain and the cytoplasmic tail, which anchors the receptor to the membrane via glycosylphosphatidylinositol (GPI) (GPI-TLR8, 45–843 a.a.) (Fig. 2A). When transiently expressed in HEK293FT cells, these mutant proteins were expressed with the expected molecular weight (Fig. 2B). Immunofluorescence staining of HeLa transfectants with anti-FLAG mAb showed that both delTIR and delCYT were displayed on the cell surface (Fig. 2C), while GPI-TLR8 resided only in the ER (Fig. 2C). The lack of expression of GPI-TLR8 on the cell surface was confirmed by flow cytometric analysis with an anti-FLAG mAb (Fig. S1). These results suggest that both transmembrane and the TIR domains are required for proper targeting of human TLR8 to the early endosome.

UNC93B1 physically associates with human TLR8

The ER membrane protein UNC93B1 interacts with TLR3, TLR7, and TLR9 in the ER through the transmembrane domain, and is critical for signaling by these TLRs. Imaging analyses revealed that UNC93B1 regulates intracellular trafficking and endolysosomal targeting of TLR7 and TLR9 [25]. However, its participation in TLR8 localization and signaling remains unknown. To determine the role of UNC93B1 in TLR8 function, we constructed an additional two TLR4/8 chimeric receptors and examined physical interaction between human UNC93B1 and wild-type TLR8, TLR4/8 chimeric receptors, or tail-truncated mutants using co-immunoprecipitation analysis. Chimera TLR4ecto/8 comprised the extracellular domain of TLR4 and the transmembrane and cytoplasmic regions of TLR8, while chimera TLR4/8TIR was composed of the extracellular, transmembrane, and linker regions of TLR4 and the TIR domain of TLR8 (Fig. 3A). As shown in Figure 3B, wild-type TLR8 protein co-immunoprecipitated with UNC93B1 protein in HEK293FT cell lysates, similar to the TLR3 protein. In addition, the TLR4ecto/8 chimeric protein, but not TLR4 and TLR4/8TIR proteins, physically associated with UNC93B1, indicates that the transmembrane region of TLR8 is required for interaction with UNC93B1 (Fig. 3B). Consistent with these results, the TLR8 mutant delCYT associated with UNC93B1, while GPI-TLR8 failed to interact with UNC93B1 (Fig. 3C).

UNC93B1 colocalizes with surface-expressed TLR8 mutants

Since delTIR and delCYT appeared on the cell surface (Fig. 2C), we next examined whether UNC93B1 translocates from the ER to the plasma membrane when these mutants were forcibly expressed in HeLa cells. Interestingly, confocal imaging analysis clearly demonstrated that endogenous UNC93B1 was colocalized with delTIR and delCYT at the plasma membrane, whereas wild-type TLR8 colocalized with UNC93B1 intracellularly (Fig. 4A).

Notably, delTIR and delCYT mutants performed as a dominant-negative against wild-type TLR8. As illustrated in Figure 4B, TLR8-mediated NF-κB activation induced with the TLR8 ligand, CL075 (a thiazoloquinolone derivative), was inhibited by the expression of either delTIR (Fig. 4B, upper graph) or delCYT (Fig. 4B, middle graph) in a dose-dependent manner. In contrast, the expression of GPI-TLR8 did not affect CL075-induced NF-κB activation mediated by wild-type TLR8 (Fig. 4B, lower graph). Thus, the delTIR and delCYT mutants appeared to interfere with the exit of wild-type TLR8 from the ER. Indeed, there was minimal overlay of wild-type TLR8 with EEA1 when co-expressed with these mutants (Fig. S2).

UNC93B1 is essential for TLR8-mediated signaling

Next, we investigated whether UNC93B1 was involved in TLR8-mediated signaling. CL075-induced TLR8-mediated NF-κB activation was greatly increased by the co-expression of UNC93B1 (Fig. 5A). Inversely, knockdown of endogenous UNC93B1 in HEK293 cells downregulated CL075-induced TLR8-mediated NF-κB activation (Fig. 5B). Thus, UNC93B1 is indispensable for TLR8 signaling.

Given that signaling via TLRs 3, 7, and 9 was disrupted in 3d mice, which expresses a UNC93B1 missense mutant (H412R) incapable of TLR binding [29], we constructed a human UNC93B1 mutant, hUNC93B1(H412R), and examined its ability

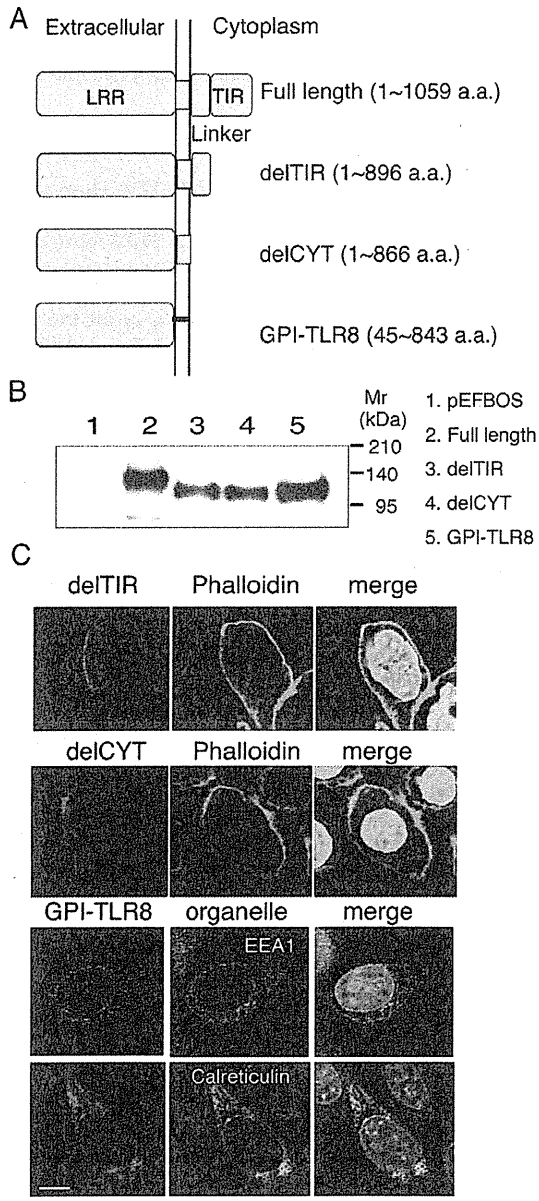

Figure 2. Defining the TLR domain responsible for localization. *A*, Schematic diagram of the tail-deletion constructs of hTLR8. *B*, Expression of the TLR tail-deletion constructs in HEK293FT cells. Wild-type and mutant proteins transiently expressed in HEK293FT cells were immunoprecipitated with anti-FLAG mAb, resolved using SDS-PAGE, and detected using immunoblotting with anti-FLAG mAb. Molecular weight markers are shown on the right. *C*, Immunofluorescence images of the TLR8 deletion constructs in transfected HeLa cells. The upper and middle panels show cells stained with delTIR and delCYT together with phalloidin, which labels the plasma membrane. The lower two panels show cells stained with GPI-TLR8 together with EEA1 or calreticulin. Green, TLR8 mutants; red, organelles; blue, nuclei stained with DAPI; bar, 10 μm.
doi:10.1371/journal.pone.0028500.g002

to bind to TLR8 and mediate signaling. hUNC93B1(H412R) failed to interact with human TLR8, similar to human TLR3 (Fig. 6A). Additionally, forced expression of hUNC93B1(H412R) did not augment CL075-induced TLR8-mediated NF-κB activation (Fig. 6B), suggesting that association of human UNC93B1 with TLR8 through His412 is required for TLR8-mediated signaling as was observed with mouse UNC93B1.

Discussion

Nucleotide-sensing TLRs are divided into two groups based on their distribution profiles in DCs. In humans, TLR3 and TLR8 are expressed in myeloid DCs, while TLR7 and TLR9 are expressed in plasmacytoid DCs [6]. Although TLR8 belongs to the TLR7/8/9 subfamily, the present study demonstrated that TLR8 possesses properties distinct from those of TLR7 and TLR9. First, TLR8, like TLR3, is localized to the early endosome but not in the late endosome/lysosome, where TLR7 and TLR9 reside. Second, although TLR8 requires UNC93B1 to exit from the ER, the TIR domain determines the endosomal targeting of TLR8.

In mouse macrophages and DCs, TLR7 and TLR9 exit the ER and travel to endolysosomes where the ectodomains of both proteins are cleaved to generate functional receptors [26,27]. UNC93B1 controls intracellular trafficking of TLR7 and TLR9 [25,28]. It is obvious that UNC93B1 physically interacts with TLR3, TLR7, and TLR9 in the ER through the transmembrane domain, and is critical for signaling of these TLRs in mice [24,29]. However, prior to this study, it was unclear whether UNC93B1 was involved in TLR8-mediated signaling. We demonstrated the interaction of human UNC93B1 with human TLR8 using a co-immunoprecipitation assay and showed that the up-regulation of TLR8-mediated NF-κB activation in HEK293 cells was induced by the ectopic expression of UNC93B1 (Figs. 3 and 5). The H412R mutation within the transmembrane domain of UNC93B1 disrupted interaction between UNC93B1 and TLR8, and thus failed to increase TLR8-mediated signaling (Fig. 6). Finally, knockdown analysis revealed that UNC93B1 is indispensable for TLR8-mediated signaling (Fig. 5B).

Although UNC93B1 has been shown to deliver TLR7 and TLR9 to endolysosomes where the receptors are cleaved by proteases, this is not the case for TLR8 or TLR3. Gibbard et al. showed that the intact ectodomain of human TLR8 is necessary for dimerization of the receptor and induction of NF-κB activation in response to a synthetic ligand, CL075, in monocytes and HEK293 cells [30]. Hence, TLR8 seems to differ from TLR7 and TLR9 in its mode of ligand recognition. Interestingly, confocal analysis of TLR8 tail-truncated mutants demonstrated that endogenous UNC93B1 moved from the ER to the plasma membrane with the TLR8 mutants. In wild-type TLR8, the TIR domain controls the targeting of TLR8 to the early endosome, although UNC93B1 is required for TLR8 exit from the ER.

The nucleotide-sensing TLRs use different regulatory elements for intracellular localization. In the case of mouse TLR7 and TLR9, the transmembrane domain determines the intracellular localization of the receptor. However, Leifer et al. reported that the cytoplasmic tail of human TLR9 controls intracellular localization [31]. A 14-amino acid region in the hTLR9-TIR domain targets the Tac (human CD25)-TLR9 chimeric receptor to early endosomes. Additionally, a recent report demonstrated that bovine TLR8 localized to the ER, and that multiple regions, including ectodomain, transmembrane, linker, and TIR regions of bovine TLR8, are involved in determining the intracellular localization [32]. Thus, there may be species-specific regulatory mechanisms of intracellular localization of TLRs.

The mechanism by which TLR8 is retained in the early endosome is currently unknown. It is likely that an unidentified

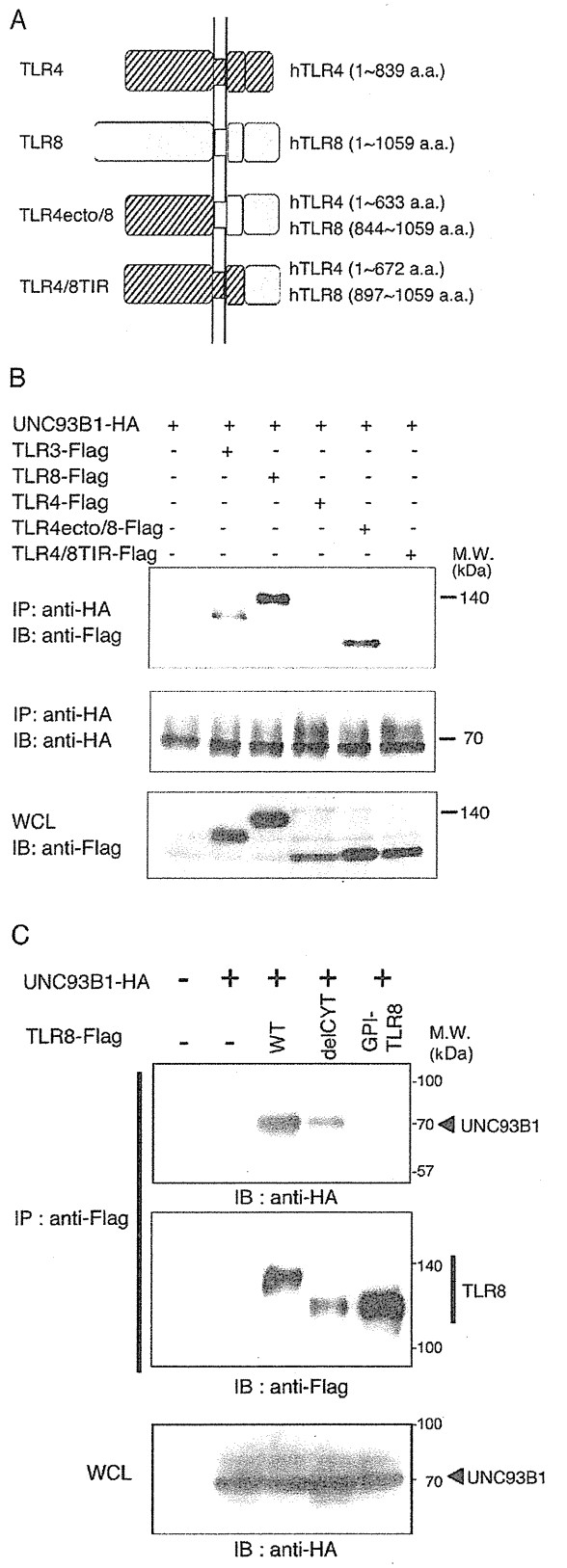

Figure 3. UNC93B1 physically associates with TLR8 through the transmembrane domain in HEK293FT cells. *A*, Schematic diagram of the TLR4/8 chimeric receptor constructs. *B, C*, HEK293FT cells were transfected with the corresponding vectors for expression of the indicated proteins. Twenty-four hours after transfection, cells were lysed in lysis buffer. The lysates were immunoprecipitated (IP) with anti-HA pAb (*B*) or anti-FLAG pAb (*C*), resolved using SDS-PAGE, and detected using immunoblotting (IB) with anti-FLAG M2 mAb or anti-HA mAb. Whole cell lysates (WCL) were subjected to immunoblotting with anti-FLAG mAb (*B*) or anti-HA mAb (*C*) to detect protein expression. Molecular weight markers are shown on the right.
doi:10.1371/journal.pone.0028500.g003

molecule interacts with the TIR domain of TLR8 and facilitates its trafficking to the early endosomes. As the BB loop in the TLR-TIR domain is critical for interaction with adaptor proteins, another region of the TLR8-TIR may participate in the association with the protein(s) regulating the receptor trafficking and intracellular localization of TLR8.

In humans, TLR7 and TLR8 recognize sequence-specific ssRNA and imidazoquinoline compounds in distinct cells and organelles, resulting in the induction of different immune responses via the same adaptor protein, MyD88. TLR7 ligands induce IFN-α production by plasmacytoid DCs, while TLR8 ligands induce proinflammatory cytokine production (e.g., TNF-α and IL-6) by myeloid DCs and monocytes [13]. This implies that TLR7 and TLR8 play distinct roles in the anti-viral immune response. Myeloid DCs express the viral RNA sensors, TLR3 and TLR8, on the endosomal membrane where they recognize virus-derived dsRNA and ssRNA, respectively. Activation of TLR3 by dsRNA results in the production of T helper 1 cytokines, such as IFN-α/β and interleukin (IL)-12p70, as well as DC maturation leading to the activation of cytotoxic T lymphocytes and natural killer (NK) cells [33]. TLR3 activation also induces TICAM-1-dependent gene expression in myeloid DCs, which mediates DC–NK reciprocal activation through cell–cell contact independently of type I IFN and IL-12 [34], whereas the key role of TLR8-mediated myeloid DC activation remains poorly understood. Detailed analyses of TLR8-mediated signaling in different cell types may give us new insight into the function of TLR8 in the anti-viral response.

Materials and Methods

Cell culture and reagents

HEK293 cells were maintained in Dulbecco's Modified Eagle's medium low glucose (Invitrogen) supplemented with 10% heat-inactivated FCS (BioSource Intl., Inc.) and antibiotics. HEK293FT cells were maintained in Dulbecco's Modified Eagle's medium high glucose supplemented with 0.1 mM NEAA, 10% heat-inactivated FCS and antibiotics. HeLa cells were maintained in Eagle's MEM (Nissui, Tokyo, Japan) supplemented with 1% L-glutamine and 10% heat-inactivated FCS. Human monocytes were isolated from peripheral blood mononuclear cells obtained from healthy individuals with a magnetic cell sorting system using anti-CD14-coated microbeads (Miltenyi Biotec, Gladbach, Germany). Anti-FLAG M2 monoclonal antibody (mAb), anti-HA polyclonal Ab (pAb), 4′,6-diamidine-2′-phenylindole dihydrochloride (DAPI), TRITC-labeled anti-phalloidin Ab, and saponin were purchased from Sigma-Aldrich. In addition, the following antibodies were used in this study: Alexa Fluor-conjugated secondary antibodies (Invitrogen), anti-HA mAb (Covance), anti-early endosome antigen 1 (EEA1) pAb (Affinity Bioreagents), anti-calnexin pAb and anti-calreticulin pAb (Stressgen, Victoria, Canada), anti-p115 pAb (Calbiochem, Darmstadt, Germany),